

Scotland's Rural College

Dual Role is Always Better than Single: Ionic Liquid as a Reaction Media and Electrolyte for Carbon-Based Materials in Supercapacitor Applications

Sheoran, Karamveer; Kaur, Harjot; Siwal, Samarjeet Singh; Thakur, Vijay Kumar

*Published in:*

Advanced Energy and Sustainability Research

*DOI:*

[10.1002/aesr.202300021](https://doi.org/10.1002/aesr.202300021)

First published: 26/04/2023

*Document Version*

Publisher's PDF, also known as Version of record

[Link to publication](#)

*Citation for published version (APA):*

Sheoran, K., Kaur, H., Siwal, S. S., & Thakur, V. K. (2023). Dual Role is Always Better than Single: Ionic Liquid as a Reaction Media and Electrolyte for Carbon-Based Materials in Supercapacitor Applications. *Advanced Energy and Sustainability Research*. <https://doi.org/10.1002/aesr.202300021>

#### **General rights**

Copyright and moral rights for the publications made accessible in the public portal are retained by the authors and/or other copyright owners and it is a condition of accessing publications that users recognise and abide by the legal requirements associated with these rights.

- Users may download and print one copy of any publication from the public portal for the purpose of private study or research.
- You may not further distribute the material or use it for any profit-making activity or commercial gain
- You may freely distribute the URL identifying the publication in the public portal ?

#### **Take down policy**

If you believe that this document breaches copyright please contact us providing details, and we will remove access to the work immediately and investigate your claim.

# Dual Role is Always Better than Single: Ionic Liquid as a Reaction Media and Electrolyte for Carbon-Based Materials in Supercapacitor Applications

Karamveer Sheoran, Harjot Kaur, Samarjeet Singh Siwal,\* and Vijay Kumar Thakur\*

The burgeoning energy demand necessitates the demand for alternative sources of energy worldwide. The development and enhancement of energy storage devices are the main focus of researchers for sustainable energy production. Carbon supercapacitors have the potential applicability as a commercial source of power. Carbon-based materials have been synthesized by utilization of ionic liquids (ILs). ILs exhibit unique properties, making them valuable materials to be utilized as a precursor, template, reaction media, and electrolytes for forming carbon-based materials and enhancing supercapacitors (SCs) performance. This review article provides detailed information about ILs in the field of SCs. First, different attractive properties are illustrated, and then the role of ILs in producing carbon-based materials in the SCs field is described. The next part provides detailed information regarding the utilization of ILs as electrolytes in carbon-based SCs. Further, the implementations of ILs as electrolytes in different carbon-based materials (such as activated carbon, graphene carbon nanotubes, and carbon nanofibers) in SCs are listed. Lastly, the importance of IL-based materials from other materials and future prospects are provided to the readers, which helps further improve the sustainable development of SCs.


because of their fast charge-discharge mechanism. These features make SCs potential candidates for power sources in portable electrical devices and electric vehicles, escalators, computer power back-ups, etc. The mechanism of SCs involves oxidation–reduction reactions in the case of electrochemical double-layer capacitance and charge transfer between electrolyte and electrode in the case of pseudo-capacitance.<sup>[2]</sup> The SC with double-layer capacitance has a longer life span, rapid charge-discharge rate, and high-power density. The SC with pseudo-capacitance can store more charge than the former due to reversible electron transfer reaction but have a lower life span. To overcome these limitations, electrode material and the electrolyte play crucial role in the designing and the performance of SCs. Interaction between the electrolyte and the electrode material surface can enhance or reduce the performance of SCs in terms of capacitance, stability, and safety. Therefore,

## 1. Introduction

The energy crisis increases worldwide due to environmental degradation coupled with fossil fuel depletion, global warming, and a rapidly surging population that necessitates the urgent demand for sustainable development of energy storage devices.<sup>[1]</sup> Among various energy storage devices, SCs attract researchers' interest due to their outstanding characteristics, such as long lifecycle, easy and cost-effective preparation, and high-power density

by optimizing the electrolyte and electrode's surface with suitable surface chemistry and tunable physiochemical properties, sustainable development in SCs can be obtained. Carbon-based materials such as activated carbon (AC),<sup>[3]</sup> carbon nanotubes (CNTs),<sup>[4]</sup> graphene and its derivatives,<sup>[5]</sup> carbon nanofibers (CNFs),<sup>[6]</sup> and others<sup>[7]</sup> are one of the most commonly utilized electrode materials for SCs owing to versatile forms such as nanotubes, fibers, powders, foils, and composites and exhibits high surface area and flexible pore size for adaption of different sized ions.<sup>[8]</sup>

K. Sheoran, H. Kaur, S. S. Siwal  
Department of Chemistry  
M.M. Engineering College  
Maharishi Markandeshwar (Deemed to be University)  
Mullana-Ambala, Haryana 133207, India  
E-mail: samarjeet6j1@mumullana.org

 The ORCID identification number(s) for the author(s) of this article can be found under <https://doi.org/10.1002/aesr.202300021>.

© 2023 The Authors. Advanced Energy and Sustainability Research published by Wiley-VCH GmbH. This is an open access article under the terms of the Creative Commons Attribution License, which permits use, distribution and reproduction in any medium, provided the original work is properly cited.

DOI: 10.1002/aesr.202300021

V. K. Thakur  
Biorefining and Advanced Materials Research Center  
Scotland's Rural College (SRUC)  
Kings Buildings, Edinburgh EH9 3JG, UK  
E-mail: Vijay.Thakur@sruc.ac.uk

V. K. Thakur  
School of Engineering  
University of Petroleum & Energy Studies (UPES)  
Dehradun, Uttarakhand 248007, India

V. K. Thakur  
Centre for Research & Development  
Chandigarh University  
Mohali, Punjab 140413, India

Carbon-based materials are used as electrode material and as catalysts or catalyst support. The development in the synthetic procedure of carbon materials with desirable properties is of significant importance.<sup>[9]</sup> ILs are potential candidates for producing carbon materials with controllable porosity and doping abundant heteroatoms within carbon materials.<sup>[10]</sup> It is reported that ILs can liquify biomass to form film materials and synthesize carbon-based materials from biomass. Studies have shown that ILs serve the role of both the templates and the stabilizer and solvent to convert biomass into porous carbon.<sup>[11]</sup>

In the case of electrolytes, organic solvents such as propylene carbonate or acetonitrile are utilized as they can operate at 2.7–3.0 V. However, these conventional organic solvents are volatile, flammable, and toxic, which can be dangerous in some situations like overpotential.<sup>[12]</sup> In 1992, Wilkes discovered air and water-stable ILs, later recognized within the community of advanced multifunctional materials.<sup>[13]</sup> ILs are attracting the focus of researchers during the past couple of years as green solvents or electrolytes owing to flexible and novel physiochemical features such as they have a melting point of less than 100 °C, and most of the ILs are liquids at room temperature (nearly 20 °C).<sup>[14]</sup> For energy storage devices, ILs have been utilized as an electrolyte and precursor for the fabrication of high-responding electrodes because of their broad electrochemical window, flameproof, distinguishing microstructure, thermal stability, and lower vapor pressure.<sup>[15]</sup>

This review paper describes the general outline, the role of ILs in carbon-based SC, and the types of ILs. Then, we elucidate the role of ILs as a precursor for the fabrication of carbon-based material with further explanation of their application in SCs. In addition, we provide a detailed overview of the utilization of ILs as electrolytes and their performance for SCs with different carbon-based materials as electrodes. Further, the applications of ILs as electrolytes in carbon-based materials for SC have been discussed. Finally, in the last section, we conclude the article

by providing future aspects of ILs in SCs having carbon-based materials as their electrodes.

## 2. General Outline and the Role of Ionic Liquids in Carbon-Based SC

In progressive SC appliances, new carbon materials incorporated with various metal oxides or conducting polymers have been used as electrodes. Researchers have recently presented MXenes and chalcogenide-based substances into electrodes for SCs.<sup>[16]</sup> The design and the constructed form of materials into the electrodes specify the capacitance, energy/power density, rate ability, and enduring steadiness of SC devices. Constant study efforts have been applied to design electrode substances possessing nano-sized pores. The objective is to improve the specific exterior area, efficiently permitting electrolytes and shrinking ionic diffusion lengths to enhance the activity of SCs.<sup>[17]</sup> In 1914, Paul Walden synthesized<sup>[18]</sup> ethyl ammonium nitrate, the first low melting salt (12 °C) and was considered the initial IL. ILs are prepared by combining cations and anions through different types of bonds. Therefore, by using a specific type of cations and anions and introducing different substances such as polymers and composites, we can customize the properties of ILs per our requirements. Some common anions and cations used to prepare ILs are shown in **Figure 1**.<sup>[19]</sup>

The electrolyte's significant role is in maintaining the life cycle, specific capacity, stability, and safety of energy storage devices. The chances of parasitic side reactions can be mitigated using appropriate electrolytes, which ultimately results in maximum output. It is reported that the pronounced enhancement in energy storage devices can be achieved using electrolytes with decent ionic conductivity and a vast potential window.<sup>[20]</sup> The physiochemical properties of ILs are directed by the structural design of ILs, which is one of the advantages of ILs for self-assembly in SCs. Besides this, ILs are environmentally and

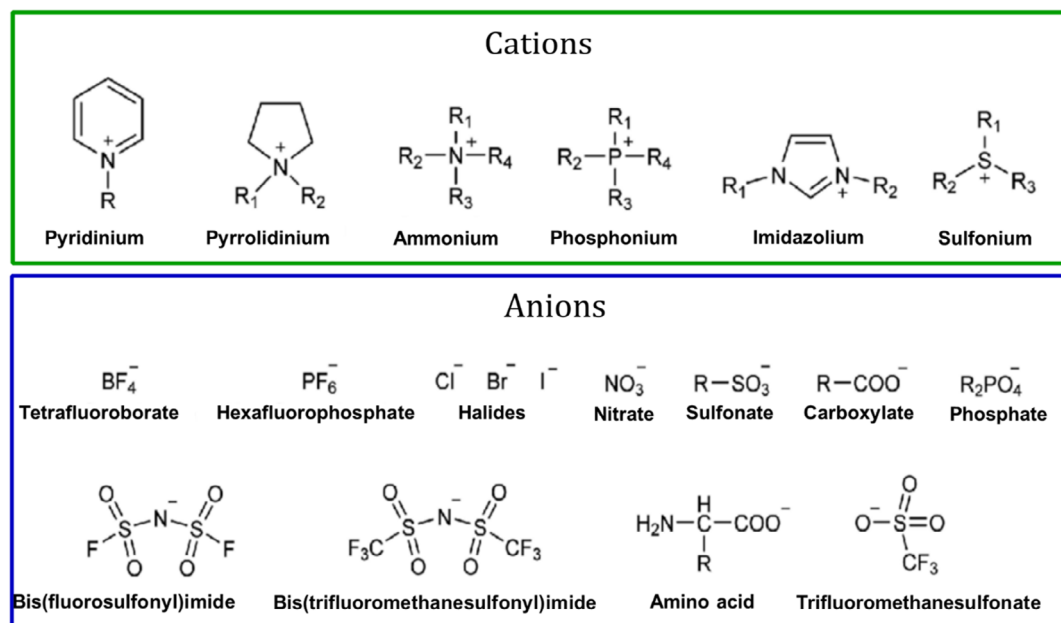


**Figure 1.** Common cations and anions are utilized for the preparation of ILs. Reprinted with permission.<sup>[19]</sup> Copyright 2021, MDPI.

ecologically friendly due to biodegradability and recyclability. Therefore, ILs are suitable electrolytes for energy storage devices in terms of life cycle and the safety of the devices.

Carbon-based materials have been utilized to improve the specific capacitance of SCs, owing to their porosity and high surface area. However, for the optimization of the operating voltage and the overall performance of the SC, electrolytes also contribute crucially regarding conductivity and interfacial capacitance, which are directly affected by the viscosity of the electrolytes.<sup>[21]</sup> The most utilized IL families as prospective electrolytes for SCs are imidazolium, pyrrolidinium (Pyr) and quaternary ammonia-based cations. Generally, imidazolium-based ILs have lesser viscosities, making them highly conductive in nature and a desirable characteristic for rapid charge–discharge cycles. Conversely, Pyr-based IL has more stability against oxidation and reduction reactions, whereas ammonia-based ILs exhibit a larger electrochemical stability window. However, Pyr and imidazolium-based ILs offer high capacitance to the cell.<sup>[22]</sup> Anions of ILs also influence the performance of SCs. Fluorides such as BF<sub>4</sub> and PF<sub>6</sub> provide more capacitance than other anions because they fit into the pore size of carbon-based nanomaterial-based electrodes of SCs. Meanwhile, ILs can also act as supporting electrolytes in solvent-based electrolytes. In the case of supporting electrolytes, ILs provide anions and cations for charge transport same as other salts provide. Compared to pure ILs, IL-solvent mixtures offer a wide range of operating voltage and higher electrical conductivity. But the thermal stability of IL-solvent electrolytes is less, i.e., they have a narrower temperature range due to conventional solvents. Therefore, for utilizing IL-solvent mixtures as an electrolyte in SCs, one must identify temperature limits for the sake of the stability of the system. The flammability of organic solvents also adds risk in the applications of IL-solvent mixtures.<sup>[23]</sup> The mixing of ILs is not limited to conventional solvents; eutectic mixtures of ILs have also been utilized as electrolytes in SCs.<sup>[24]</sup> The properties of ILs are described in **Figure 2** along with their applications in SCs where carbon-based electrodes are utilized as electrodes.

The characteristics mentioned above of ILs are also beneficial for forming new materials, which opens new paths in material chemistry. Carbon-based materials have been synthesized from

ILs. Initially, ILs were utilized as templates for producing carbon-based materials and later they were recognized as suitable porosity-directing regulators and reaction media for converting biomass into porous carbon-based materials.<sup>[9a,25]</sup> In the next section, we shed light on the aspects of ILs in forming carbon-based materials.

### 3. Ionic Liquids as Advanced Reaction Media to Synthesize Carbon-Based Materials and Their Performance in Supercapacitors

Carbon materials have been fascinating materials for supercapacitors due to various microstructures, interconnected pore size, good wettability for electrolytes, high surface area, and stable surface functionalities.<sup>[26]</sup> Different carbon-based materials for SCs application are described in **Figure 3**. The addition of heteroatom practical groups upon the exterior of carbon material further enhances the material's reactivity. Several methods have been made to fabricate carbon-based materials with desired functional groups.<sup>[27]</sup> Usually, pyrolysis is carried out using polymers or raw biomass to prepare carbon-based materials.<sup>[28]</sup> It can introduce

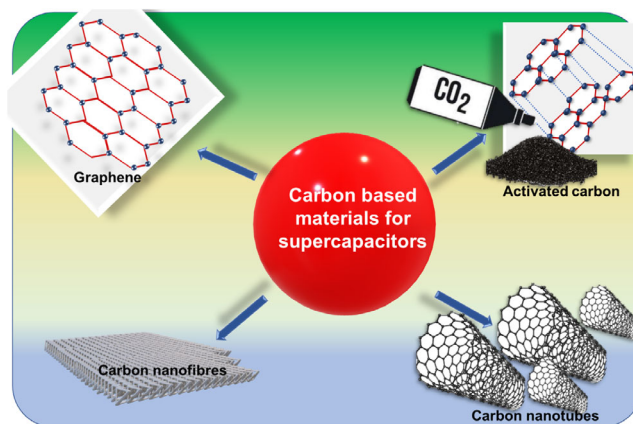


**Figure 3.** Different carbon-based materials are utilized in SCs.

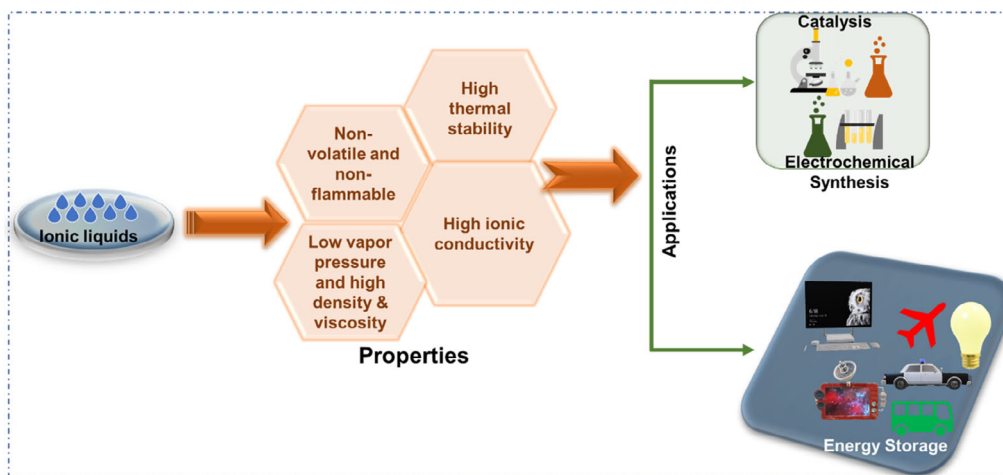


**Figure 2.** Properties of ILs along with their applications in SCs where carbon-based electrodes are utilized as electrodes.

heteroatoms into carbon materials by treating carbon material with reactive gases like  $\text{H}_2\text{S}$  and ammonia or by carbonizing heteroatom-containing polymers.<sup>[9a]</sup> Owing to attractive characteristics such as low volatilities and flammability, carbon-rich nature, high thermal and electrochemical stability, versatile combination of cations and anions, low toxicity etc., ILs have been utilized as precursors or reaction media for the synthesis of carbon-based materials. Compared to other techniques, ILs offer a more straightforward carbonization procedure.<sup>[8a]</sup> Porous carbon materials can be synthesized by ionothermal carbonization, where ILs act as reaction media<sup>[29]</sup> or via direct carbonization, where ILs are utilized as precursors.<sup>[30]</sup>

Various studies reported that ILs had been utilized as templates for producing carbon-based materials used as SC electrodes. For instance, a team of researchers fabricated CNT/N-doped mesoporous carbon by utilizing IL (1-alkyl-3-methylimidazolium bromide) as a nitrogen source and template for the carbon source they utilized resorcinol-formaldehyde and as an assistant agent, tetraethyl orthosilicate was used. This material was used as an SC electrode and provided decent specific capacitance of  $244 \text{ F g}^{-1}$ . It was modifying CNTs with 1-alkyl-3-methylimidazolium bromide results in a higher dispersion degree of CNTs as IL forms interweaved networks via surface electrostatic interactions. The synthesized material exhibits a surface area of  $857 \text{ m}^2 \text{ g}^{-1}$  and a pore volume of  $0.79 \text{ cm}^3 \text{ g}^{-1}$ . SC displayed high stability as it showed a retention capacity of nearly 92% after 5000 cycles.<sup>[31]</sup> The sol-gel technique was utilized to synthesize carbon xerogels, where 1-butyl-3-methylimidazolium tetrafluoroborate was employed as a template. The synthesized substance had a specific surface area of  $2391 \text{ m}^2 \text{ g}^{-1}$  and decent stability after 12 500 charge/discharge cycles.<sup>[32]</sup>

Furthermore, ILs have been utilized as precursors, such as nitrogen-doped porous carbon fabricated from 1-butyl-3-methylimidazolium dicyanamide by carbonization process where mesoporous silica was utilized as a template.<sup>[33]</sup> The prepared substantial was applied as an SC electrode, and the system exhibited stability of 95% after 1000 cycles. Temperature played a vital character in the prepared material's morphology as the surface area increased with the increased temperature. The obtained material had a specific area of  $931 \text{ m}^2 \text{ g}^{-1}$  and a specific capacitance of  $210 \text{ F g}^{-1}$ . Further, for developing nitrogen and oxygen-doped porous carbon material, Li Z. et al.<sup>[34]</sup> utilized carboxymethyl-based protic polyanion ILs as a precursor. The carbonization technique followed by KOH activation of ILs was used to prepare the material. A specific exterior area of  $3757 \text{ m}^2 \text{ g}^{-1}$  was observed. When this substance was utilized as the electrode of the SC, high electrochemical performance was obtained with cycling stability of nearly 99% after 10 000 cycles, a capacitance of  $291 \text{ F g}^{-1}$ , and a power density of  $26 \text{ W kg}^{-1}$  corresponding to the energy density of  $10.11 \text{ Wh kg}^{-1}$ . Phosphoric acid protic IL of arginine was used as a precursor for synthesizing nitrogen and phosphorous-doped porous carbon material.<sup>[35]</sup> The device had a stability of 94% after 10 000 cycles, a surface area of  $751 \text{ m}^2 \text{ g}^{-1}$ , and a specific capacitance of  $170 \text{ F g}^{-1}$ .

Zhou H. et al.<sup>[36]</sup> incorporated nitrogen-sulfur-doped porous carbon material via direct carbonization of amino-acid protic ILs. The authors observed that aromatic amino-acid ILs yield more carbon than aliphatic and heterocyclic morphology. Thus, carbon material formed from lysine (Lys) and tryptophan (Trp)

was triggered via  $\text{NH}_4\text{Cl}$ , KOH, and  $\text{K}_2\text{CO}_3$ , correspondingly. And the surface appearance of the Lys, Lys- $\text{NH}_4\text{Cl}$ , Lys-KOH, and Lys- $\text{K}_2\text{CO}_3$  was defined through SEM image, as shown in **Figure 4a–d**. It can be observed Lys's loose laminated structure within **Figure 4a**. **Figure 4b–d** demonstrates the corresponding porous carbons with an enormous amount of interface for charge storage acquired through activation. It may notice the large interconnected pores network frameworks in **Figure 4b**, showing the prosperous "gas escaping channels" influenced by  $\text{NH}_4\text{Cl}$ . **Figure 4e** illustrates the CV arcs of Lys, Lys- $\text{NH}_4\text{Cl}$ , Lys-KOH, and Lys- $\text{K}_2\text{CO}_3$  probes on the sweep rate of  $100 \text{ mV s}^{-1}$ , that is calculated within a voltage range of  $-1-0 \text{ V}$ . It is essential mentioning that Lys- $\text{K}_2\text{CO}_3$  showed the main rectangular-designed site between the probes, showing the perfect electric capacitance owing to the most elevated  $S_{\text{BET}}$  with micropores and mesopores. On the other side, Lys showed the most negligible double-layer capacitance, ascribed to the little exact area only with narrow micropores. The distinctive GCD curves of the specimens at  $1 \text{ A g}^{-1}$  are illustrated in **Figure 4f**, indicating an isosceles triangle form, although insufficient balance. The obtained specific capacitance of the four conductors concerning the CD curves is shown in **Figure 4g**, which delivered a higher specific capacitance than the reported carbon materials. Furthermore, the electrochemical activity of Lys- $\text{K}_2\text{CO}_3$  is deeply studied within **Figure 4h–j**. The rectangular form of CV arcs at various sweep rates (**Figure 4h**) ensures that the ingredients have an excellent electrochemical capacitor. **Figure 4i** shows the balanced triangular GCD shapes upon a broad range from 1 to  $20 \text{ A g}^{-1}$  deprived of a substantial drop. Similarly, the long-life GCD at a current density of  $5 \text{ A g}^{-1}$  was tried and offered superior cycling resilience with nearly 100% afterwards 5000 runs (**Figure 4j**), showing outstanding electrochemical steadiness.

Now, we illustrate several studies where ILs can act as a template and precursor in generating carbon-based materials. Chao Liu et al.<sup>[37]</sup> utilized 1,3-dimethyl-imidazole dimethyl phosphate to prepare nitrogen and phosphorus-doped porous carbon microspheres. The material was made by a two-step method, as displayed in **Figure 5a**. In the preoxidation step, the IL acted as a medium, while in the carbonization procedure, the IL worked as a template. The mixture of lignin and IL provided heteroatoms to the carbon framework, where lignin worked as a carbon source, and IL worked as a dopant. The developed material's well-developed microporous and mesoporous structure was confirmed by  $\text{N}_2$  absorption-desorption isotherms and pore size circulation curves, as showcased in **Figure 5b,c**. The synthesized material had a specific surface area of  $938.1 \text{ m}^2 \text{ g}^{-1}$  with a pore volume of  $0.64 \text{ cm}^3 \text{ g}^{-1}$  and was used as SC electrode material. When ran the system at  $750^\circ\text{C}$ , the system showed the highest specific capacitance of  $338.2 \text{ F g}^{-1}$ . CV curves of the prepared material at diverse scan rates are displayed in **Figure 5d**; the curves showed that the material had a decent pace and capacitive performance. By increasing the value of current densities, the specific capacitance of the device was also increased, as demonstrated in GCD curves (**Figure 5e**). Specific capacitance along with LED light is shown in **Figure 5f**, and electrochemical impedance spectroscopic value of the device was  $0.508 \Omega$  (**Figure 5g**), which suggested the material exhibited good electrical conductivity due to lower charge transfer resistance. For the system's stability analysis, the CD test was utilized, which revealed that after

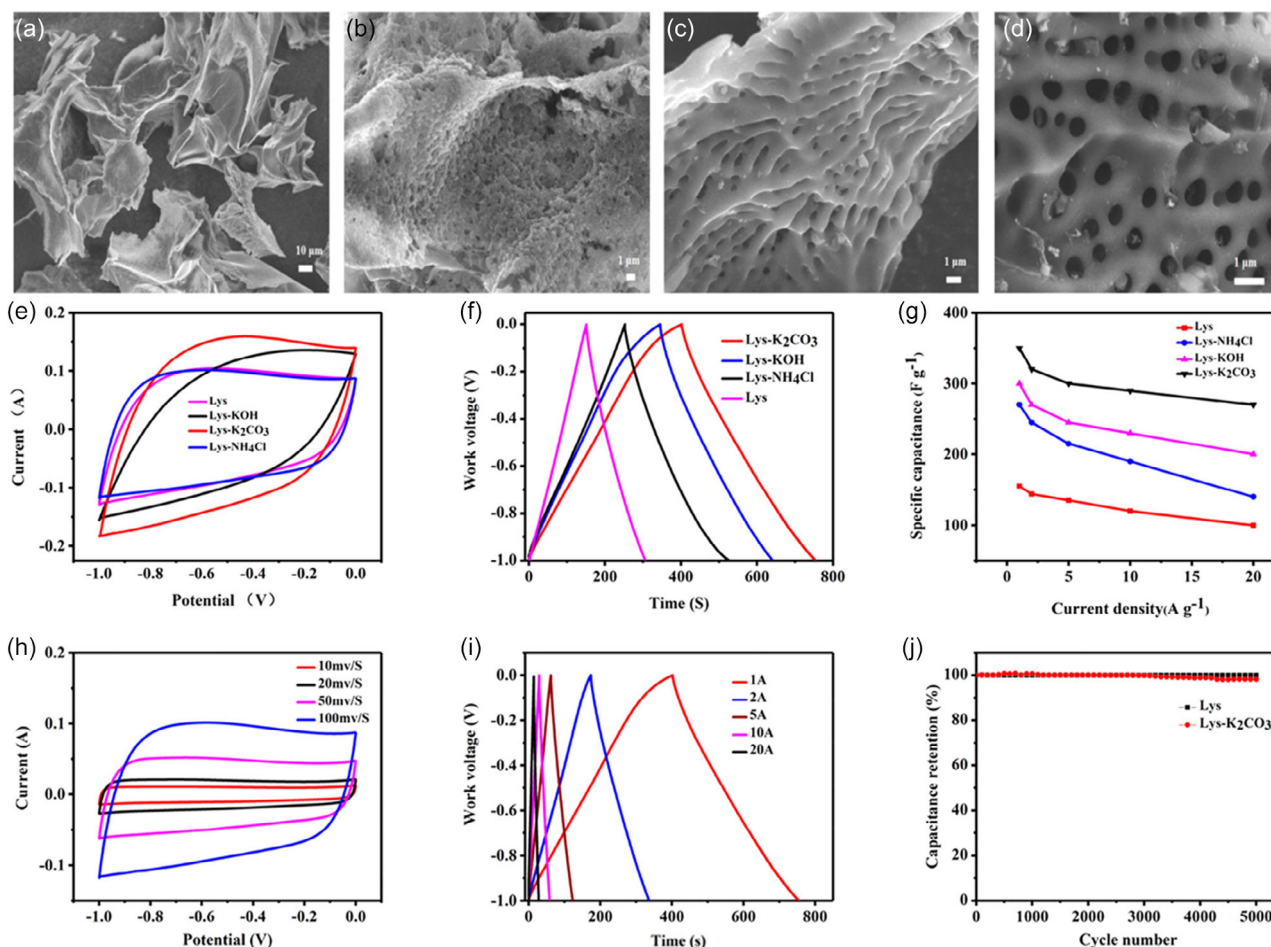


**Figure 4.** SEM pictures: a) Lys, b) Lys-NH<sub>4</sub>Cl, c) Lys-KOH, and d) Lys-K<sub>2</sub>CO<sub>3</sub>. Electrochemical presentation of the Lys, Lys-NH<sub>4</sub>Cl, Lys-KOH, and Lys-K<sub>2</sub>CO<sub>3</sub>: e) CV arcs at 100 mV s<sup>-1</sup>; f) GCD arcs below 1 A g<sup>-1</sup>; g) disparity of the specific capacitances on diverse current densities. Electrochemical activity of the Lys-K<sub>2</sub>CO<sub>3</sub>; h) CV profiles vs dissimilar sweep rates; i) GCD arcs versus diverse current densities; j) cycling presentation by repetition GCD at 5 A g<sup>-1</sup>. Reprinted with permission.<sup>[36]</sup> Copyright 2019, American Chemical Society.

5000 cycles, the system exhibited a retention capacity of 97.3% within the potential range of 0–1 V (Figure 5h). Ragone plot Figure 5i demonstrated that the system had an energy density (ED) of 7.81 Wh kg<sup>-1</sup>, corresponding to a power density (PD) of 62.5 W kg<sup>-1</sup>.

Another team of researchers synthesized nitrogen-doped porous carbon through direct carbonization of sodium lignosulfonate and 1-allyl-3-methyl imidazolium chloride-based IL,<sup>[38]</sup> where IL acts as a precursor and additional template or activation agent was not required as utilized IL was self-activating and self-templating. The obtained material showed decent performance as an SC electrode. At 700 °C, the system had a 230 F g<sup>-1</sup> capacitance and a retaining capacity of 90.3% afterward 2000 runs. It exhibited ED of 7.99 Wh kg<sup>-1</sup> with a PD of 25 W kg<sup>-1</sup>. Protic salts are considered a type of ILs produced via the neutralization of N-containing bases and acids<sup>[30]</sup> and can be utilized to prepare carbon-based materials. For instance, Miao et al.<sup>[39]</sup> developed N, S doped porous carbon nanosheets using the protic salt of p-phenylenediamine toluene sulfate, which served as a precursor and a template. This protic salt not only served as a carbon source

but also as a source of N and S. When the as-synthesized material was modified on SC's electrode, it showed high electrochemical performance involving cyclic stability of 94.4% after 10 000 cycles. The system exhibited a decent gravimetric capacitance of 280 F g<sup>-1</sup> in KOH electrolyte.

Table 1 summarizes ILs utilized as reaction media, templates, and precursors for forming carbon-based materials and their application in SCs.

#### 4. Ionic Liquids as Electrolytes in Carbon-Based Supercapacitor Application

IL-based, organic-based, and water-based solutions have been utilized as electrolytes in SCs. Some scholarly works have previously elucidated different electrolytes for SCs.<sup>[40]</sup> Water-based (aqueous) electrolytes have some limitations, such as their life cycle and energy density being less, although their power density and capacitance are high. The major demerit of water-based electrolytes is the narrow range of electrochemical stability as water is

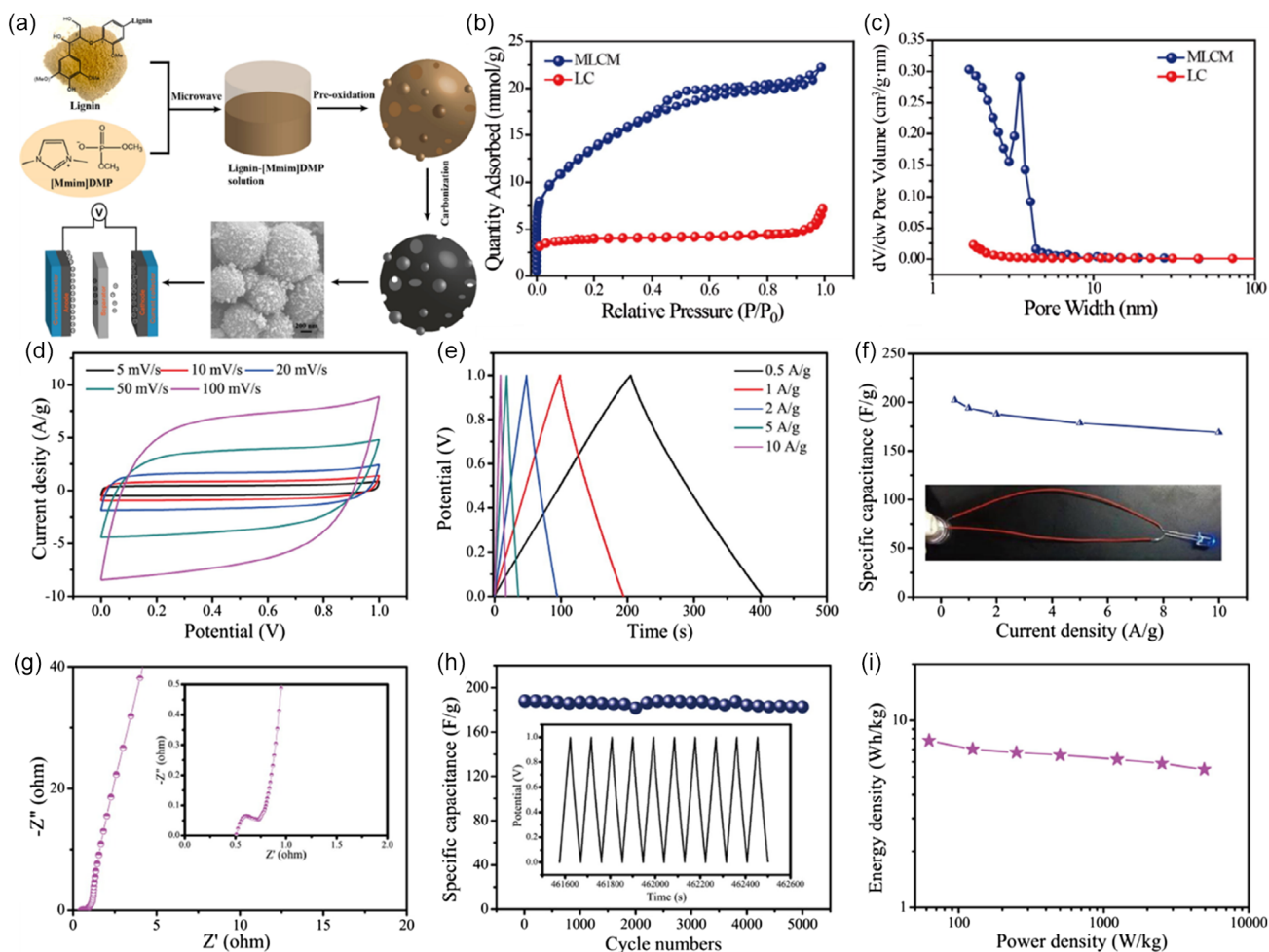


**Figure 5.** a) Graphical design of the synthetic procedure of carbon microspheres; b,c)  $N_2$  absorption–desorption isotherms with pore size distribution curves; d,e) CV and GCD curves at different scan rates; f–h) gravimetric capacitance with LED lighting in the inset, EIS spectra and stability curve of the device; i) Ragone plot for the analysis of EDs corresponding to PDs. Reprinted with permission.<sup>[37]</sup> Copyright 2022, Elsevier Ltd.

stable in the field of 1.23 V, and after the introduction of salts, can be expanded this range to 1.6–1.8 V<sup>[41]</sup> and, in some cases, can expand it up to 2.5 V<sup>[42]</sup> which is still not enough for most of the applications. Most organic electrolytes comprise the dissolution of acetonitrile/propylene carbonate and quaternary ammonium salts. The operating voltage range of organic electrolytes in commercially available SCs is 2.7–2.8 V, which cannot exceed further because of the degradation of organic solvents.<sup>[43]</sup> At the same time, ILs formed by cations and anions with melting temperatures below 100 °C have a wide range of electrochemical stability of 6 V<sup>[44]</sup> and can be utilized without solvents. Thus, they can be considered potential candidates as electrolytes in SCs.

Moreover, the required temperature for SCs to be used in military equipment is nearly –55 °C; for automotive devices, SCs should work at 125 °C, and for consumer electronics, the required temperature range is –20–85 °C.<sup>[45]</sup> Therefore, organic solvents can be dangerous due to flammability, whereas ILs are suitable electrolytes because of their thermally stable and non-flammable characteristics.<sup>[46]</sup> Further, it is revealed that the pore size of the material and the ion size of the electrolyte affect the capacitive performance of the system. The pore size should be

comparable with the size of the ions of electrolyte as too smaller pore size are ion-inaccessible while too larger pore size creates wider space between the pore wall and ions, both lead to a considerable decrease in capacitance value of the system.<sup>[47]</sup> Thus, utilizing appropriate IL electrolyte and carbon material with comparable dimensions favors the efficient capacitive performance of SCs. For instance, Song Z. et al.<sup>[48]</sup> synthesized heteroatom-doped hydrangea-like porous carbon with a pore size of 0.80 and 0.50 nm which were comparable to the ion size of the utilized ILs named EMIMBF<sub>4</sub> and EMIM bis(trifluoromethyl sulfonyl)imide with 0.76 nm size of cation while 0.48 nm for BF<sub>4</sub><sup>–</sup>. The authors observed high specific energy of 101.2 Wh kg<sup>–1</sup>. In this section, we elucidate different ionic liquids utilized as electrolytes in SCs applications where carbon-based materials are used as electrodes.

#### 4.1. Ionic Liquids as Electrolytes for Activated Carbon-Based SCs

The electrical double-layer capacitors (EDLC), established upon particular exterior area carbon probes, which work by separating charges at the electrode/media boundary, are the most developed

**Table 1.** Utilizing ILs as reaction media, template, and precursor for forming carbon-based materials and their application in SCs.

Types of ILs	Role of IL	Types of carbon materials	Preparation technique	Performance in SC	References
1,3-Dimethyl-imidazole Dimethyl Phosphate	Template and reaction media	Porous carbon materials	Direct carbonization	Exhibited ED of 7.81 Wh kg <sup>-1</sup> corresponding to PD of 62.5 W kg <sup>-1</sup> and specific capacitance of 338.2 F g <sup>-1</sup>	[37]
1-Butyl-3-methylimidazolium dicyanamide	Precursor	Nitrogen-doped mesoporous carbon	Carbonization	210 F g <sup>-1</sup> was specific capacitance and showed stability of 95% after 1000 cycles	[33]
Carboxymethyl-based protic polyanion	Precursor	Nitrogen and oxygen-doped mesoporous carbon	Carbonization	Cycling stability of nearly 99% after 10 000 cycles, capacitance of 291 F g <sup>-1</sup> and PD of 26 W kg <sup>-1</sup> corresponding to ED of 10.11 Wh kg <sup>-1</sup> was obtained	[34]
Phosphoric acid protic IL of arginine	Precursor	Nitrogen-phosphorous-doped porous carbon	Carbonization	Had a stability of 94% after 10 000 cycles	[35]
Amino-acid protic ILs	Precursor	Nitrogen-sulfur-doped porous carbon	Direct carbonization	Exhibited ED of 6.9 Wh kg <sup>-1</sup> corresponding to PD of 248 W kg <sup>-1</sup> and specific capacitance of 350 F g <sup>-1</sup>	[36]
Sodium lignosulfonate and 1-allyl-3-methyl imidazolium chloride-based IL	Precursor as well as template	Nitrogen-doped porous carbon	Direct carbonization	Had capacitance of 230 F g <sup>-1</sup> , retention capacity of 90.3% after 2000 cycles and ED of 7.99 Wh kg <sup>-1</sup> with PD of 25 W kg <sup>-1</sup>	[38]
Dilute sulfuric acid and phenothiazine-based IL	Precursor	Nitrogen-sulfur-doped porous carbon	One-step carbonization	Exhibits specific capacitance of 302 F g <sup>-1</sup> and cyclic stability of almost 100% over 5000 cycles	[81]
Alginate-based protic polyanion ILs	Precursor	Nitrogen-doped porous carbon	Carbonization followed by activation	Exhibits surface area of 3638 m <sup>2</sup> g <sup>-1</sup> , pore size of 2.44 nm, gravimetric capacitance of 354 F g <sup>-1</sup> and delivered ED of 12.3 Wh kg <sup>-1</sup> corresponding to PD of 26 W kg <sup>-1</sup> . had cyclic stability of 95% over 10 000 cycles	[82]
1-Ethyl-3-methylimidazolium dicyanamide	Precursor	Nitrogen-doped porous carbon	One-step carbonization	Showed specific capacitance of 335.3 F g <sup>-1</sup> and ED of 10.1 Wh kg <sup>-1</sup>	[83]
Task-specific ILs with dicyanamide anions	Precursor	Nitrogen-doped ordered porous carbon	Soft template strategy	Delivered high specific capacitance of 427 F g <sup>-1</sup> with nearly 98% retention capacity after 2000 runs and surface area of 1919 m <sup>2</sup> g <sup>-1</sup>	[84]
1-Vinyl-3-butylimidazolium bromide and divinylbenzene based IL	Precursor	Nitrogen-doped porous carbon	Carbonization	Delivered specific capacitance of 243 F g <sup>-1</sup> with almost 100% stability after 2400 cycles and had surface area of 1324 m <sup>2</sup> g <sup>-1</sup>	[85]
1-Butyl-3-methylimidazolium tetrafluoroborate	Template	Carbon xerogels	Sol-gel polymerization	Exhibits specific surface area of 2391 m <sup>2</sup> g <sup>-1</sup> and decent stability after 12 500 CD cycles	[32]
1-butyl-3- methylimidazolium tetrafluoroborate	Template	Graphene-carbon xerogels	–	Delivered 230 F g <sup>-1</sup> and almost no degradation after 5000 runs	[86]
Resorcinol/formaldehyde-based ILs	Template	Nitrogen-doped mesoporous carbon spheres	Sol-gel method and carbonization	Showed good capacitance of 159 F g <sup>-1</sup> and 88% stability after 5000 runs	[87]

and are already in demand. ACs are the most generally utilized electrode substances for EDLC applications owing to their moderately economical and increased surface area than other carbon materials. The possible potential of any SC appliance relies on the potential electrolyte range, where the performance depends both upon the electrode core and electrolyte characteristics; thus, selecting the electrolyte is essential.

In this regard, dimethyl thioformamide-based IL was prepared by Kong J. et al.,<sup>[49]</sup> which was utilized in AC-based SCs and exhibited higher thermal stability up to 351 °C and a decent specific capacitance of 90 F g<sup>-1</sup>. Fleischmann et al.<sup>[50]</sup> proposed alkali ion-based IL electrolytes for asymmetric hybrid SC. AC-based electrode and Li-bis(trifluoromethyl sulfonyl)imide and Na bis(trifluoromethyl sulfonyl)imide (with 99.9% purity) as

electrolytes were utilized in this system. Briefly, 1 M Li-based IL showed coulombic efficiency of 90% at 2 V and a capacity of 80 mAh g<sup>-1</sup> with a maximum capacity of 143 mAh g<sup>-1</sup>, while 0.5 M Li-based IL electrolyte obtained a specific capacity of 138 mAh g<sup>-1</sup>. The coulombic efficiency proves the compatibility of Li-based IL electrolytes. The coulombic efficiency remains 99.8% even after 200 runs, which showed that the system was highly stable in 1 M Li-based IL electrolyte. In the case of Na-based IL, 98% coulombic efficiency was obtained after 200 cycles.

Therefore, alkali ion-based ILs enhance the anodic stability, improving the specific energy. Also, the system was thermally stable up to 80 °C. ACs can be fabricated from biomass or organic wastes such as corn grains, rice husk, human hairs, dead leaves, coconut shells, and banana fibers, which is eco-friendly and can



produce many ACs that can be utilized as electrodes in energy storage devices.<sup>[51]</sup> N-doped AC was obtained from palm flowers by Sahoo and Rao,<sup>[52]</sup> when employed with IL-based electrolyte in SCs showed PD and ED of 38.9 and 8.6 Wh kg<sup>-1</sup>, correspondingly, at an operating voltage of 1.5 V and current density of 0.1 A g<sup>-1</sup>. Other researchers also derived AC from biomass, i.e., rice straw, through carbonization and activation. By utilizing 1-ethyl-3-methylimidazolium tetrafluoroborate [EMIMBF<sub>4</sub>] as an electrolyte for SC, the catalyst has a specific surface area of 1007 m<sup>2</sup> g<sup>-1</sup> that enhances the interface among electrode and electrolyte, which results in better capacitance and ED of SC. The system exhibits an ED of 17.4 Wh kg<sup>-1</sup> with a specific capacitance of 80 F g<sup>-1</sup> and a PD of 174 W kg<sup>-1</sup>.<sup>[51a]</sup>

Mesoporous AC having a fiber-like structure was fabricated by a team of researchers<sup>[53]</sup> to use as an electrode for SCs with IL-based electrolytes. Mesoporous AC fibers were synthesized via the carbonization-activation technique using polyacrylonitrile as a precursor, as showcased in Figure 6a. The obtained material exhibited ionic conductivity of 57–195 S cm<sup>-1</sup> and a surface area of 2404 m<sup>2</sup> g<sup>-1</sup>. Ions of electrolytes were diffused rapidly along the radial direction owing to the 1-dimensional fiber structure, which favors the high CD capability and better power performance of SCs. [EMIMBF<sub>4</sub>] was utilized as an electrolyte at an operating voltage of 4 V; the as-prepared system displayed energy density at 1 kW kg<sup>-1</sup> and capacitance of 113 Wh kg<sup>-1</sup> and 204 F g<sup>-1</sup> at 0.5 A g<sup>-1</sup>, correspondingly. CV curve elucidating the capacitance performance of the as-synthesized material at scan rates of 100–1000 mV s<sup>-1</sup> is shown within Figure 6b. The comparative capacitance performance of the prepared material with other materials is shown in Figure 6c. Linear response of the charge–discharge process with different current

densities can be seen from GCD curves, as showcased in Figure 6d.

In addition to this, trihexyl (tetradecyl) phosphonium bis (trifluoromethane sulfonyl) imide was utilized as an electrolyte for AC-based SC by Pilathottathil et al.<sup>[54]</sup> The authors observed that the as-synthesized material displayed high ED and specific capacitance of 110 Wh kg<sup>-1</sup> and 300 F g<sup>-1</sup>, respectively, at a working potential of 3.5 V and showed stability up to 1000 cycles.

Pyrrrolidinium (Pyrr) methane sulfonate (MeSO<sub>3</sub>) and diisopropylethylammonium MeSO<sub>3</sub> was utilized as electrolyte for AC-based SCs by Anouti et al.,<sup>[55]</sup> which exhibited a PD of 13.9 kW kg<sup>-1</sup> and specific capacitance of 102 F g<sup>-1</sup> at a current density of 15 A g<sup>-1</sup>. Timperman, L. et al.<sup>[56]</sup> utilized Pyrr with nitrate and bis(trifluoromethanesulfonyl)imide prepared via equimolar metathesis as an electrolyte for AC-based SCs. At a cell potential of 2 V, the SC showed a specific capacitance of 148 F g<sup>-1</sup>, and at 25 °C, more than 80% capacitive retention was observed up to 110 hr. Table 2 summarizes the utilization of ILs as electrolytes for AC-based SCs.

#### 4.2. Ionic Liquids as Electrolytes for Graphene and Its Derivative Based SCs

Graphene and its derivatives have high electric conductivity, wide potential windows, and large surface area, which provides high electrochemical efficiency to SC.<sup>[57]</sup> ILs enhance these characteristics of graphene-based materials, improving the overall performance of the SCs. Here, we elucidate the version of SCs with graphene and derivative-based electrodes utilizing ILs as electrolytes.

Zhu H. et al.<sup>[58]</sup> fabricated flexible IL-based SC where graphene quantum dots (GQDs) modified with MnO<sub>2</sub> were used

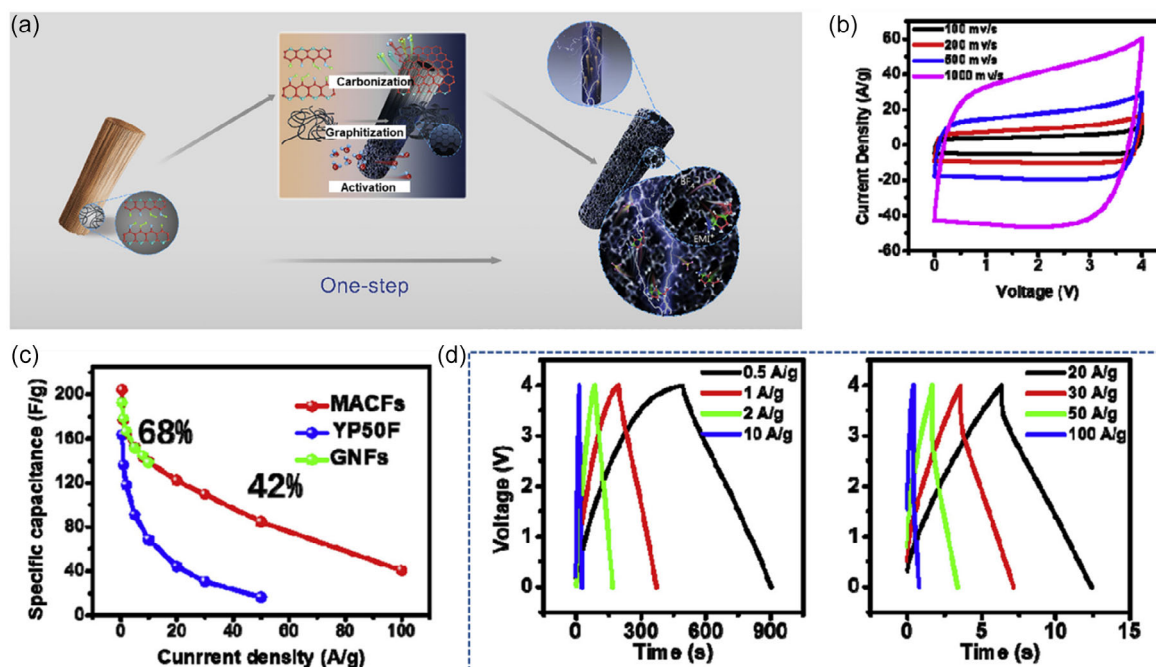


**Figure 6.** a) Graphical representation of the fabrication method of mesoporous AC fibers; b) CV curve at scan rates of 100 mV s<sup>-1</sup> to 1000 mV s<sup>-1</sup>; c) comparison of the capacitance performance of mesoporous AC fibers with other material; d) GCD arcs of the prepared material with IL as electrolyte. Reprinted with permission.<sup>[53]</sup> Copyright 2019, Elsevier Ltd.

**Table 2.** Summary of the utilization of ILs as electrolytes for AC based SCs.

Electrolyte	Electrode	Preparation technique/conditions	Cell voltage	Surface area [m <sup>2</sup> g <sup>-1</sup> ]	Specific capacitance [F g <sup>-1</sup> ]	Stability	Energy density [Wh kg <sup>-1</sup> ]	Power density [kW kg <sup>-1</sup> ]	References
EMIMBF <sub>4</sub>	Brinjal biomass derived AC	One pot chemical activation technique	–	850	133	–	41	–	[3a]
Pyrr + nitrate + bis(trifluoromethane sulfonyl)imide	AC	–	2.0	–	148	80% for 110 hr	–	–	[56]
[Pyrr][MeSO <sub>3</sub> ] and [diisoprpyethylammonium][MeSO <sub>3</sub> ]	AC	–	–	–	102	–	–	13.9	[55]
Li- bis(trifluoromethyl sulfonyl)imide	AC	–	4	–	–	99.8% after 200 cycles	98	1.9	[50]
Na- bis(trifluoromethyl sulfonyl)imide	AC	–	4	–	–	98% after 200 cycles	90	1.8	[50]
[EMIM][ESO <sub>4</sub> ]	Palm flower derived AC	Hydrothermal method	1.5	164	–	–	8.6	38.9	[52]
EMIMBF <sub>4</sub>	AC	Carbonization and activation process	4 V	2404	204	–	113	–	[53]
EMIMBF <sub>4</sub>	Rice straw derived AC	Carbonization and activation	2.5 V	1007	80	78% after 5000 cycles	17.4	174	[51a]
Tetrabutylammonium bromide	AC supported vanadomolybdates	–	1.2 V	–	146	–	29.2	1440	[88]
Trihexyl (tetradecyl) phosphonium bis (trifluoromethanesulfonyl) imide	AC	–	3.5 V	–	300	Stable up to 1000 cycles	110	–	[54]
1-Butyl-3-methylimidazolium iodide	AC	–	2 V	–	56.5	82.5% after 1000 cycles	31.39	5012.58	[89]

as electrode material prepared via the modified solvothermal method. The authors reported a decent ED of 82.2 Wh kg<sup>-1</sup>, an excellent specific capacitance of 208.2 F g<sup>-1</sup>, and a PD of 11.6 kW kg<sup>-1</sup>. Reduced graphene oxide (rGO) modified with α-MnO<sub>2</sub> fiber combined with nitrogen and sulfur (α-MnO<sub>2</sub>/N-S/rGO) was synthesized as an electrode for SC by Poochai et al.<sup>[59]</sup> where N,N-diethyl-N-methyl-N-(2-methoxy-ethyl)ammonium bis (trifluoromethyl-sulfonyl)amide IL was utilized as electrolyte material. The systematic preparation procedure is displayed in Figure 7a. Electrochemical investigation revealed that the as-synthesized material exhibits a specific capacitance of 165 F g<sup>-1</sup> at a cell voltage of 4.5 V. CV and GCD curves of the synthesized material, as showcased in Figure 7b,c, depicted that the material had an ED of 110 Wh kg<sup>-1</sup> and PD of 550 kW kg<sup>-1</sup> at a current density of 0.25 A g<sup>-1</sup>. Further, the stability of the system can be seen from graphs Figure 7d,e, with a retention capacity of approximately 96% even after 10 000 cycles. The GO-based electrode was synthesized by another team of researchers<sup>[60]</sup> for SC based on a eutectic mixture of ILs (N-methyl-N-propyl piperidinium bis (fluorosulfonyl)imide (PIP13-FSI) and N-butyl-N-methyl pyrrolidinium bis (fluorosulfonyl)imide) electrolyte. The electrode exhibits a surface area of 1901 m<sup>2</sup> g<sup>-1</sup>, and the system was stable over an extensive range of temperature (–50–80 °C). At 3.5 V, a specific capacitance of 180 F g<sup>-1</sup> was reached.

The graphene-based electrode was fabricated by dispersion technique for IL-based SC, and 1-butyl-3-methylimidazolium tetrafluoroborate was used as electrolyte.<sup>[61]</sup> The system had high ionic conductivity with a low charge transfer resistance of 0.79 Ωcm<sup>2</sup>. In addition, the electrochemical study showed that the device had a specific capacitance of 214 F g<sup>-1</sup> and energy

density of 33.3 Wh kg<sup>-1</sup> at a current density of 3 A g<sup>-1</sup> with a power density of 24.7 Wh kg<sup>-1</sup>. The GO-based electrode was synthesized using urea phosphate through one-step hydrothermal technique, and EMIMBF<sub>4</sub> was used as an electrolyte in SC.<sup>[62]</sup> Researchers observed a high ED of 97.2 Wh kg<sup>-1</sup> with 0.9 kW kg<sup>-1</sup> PD. At 1 A g<sup>-1</sup>, the device had a specific capacitance of 196.7 F g<sup>-1</sup> and a high retention capacity of 78.3% after 5500 cycles which proved the system's stability. Modified Hummer's method, followed by a one-pot hydrothermal approach, was utilized by Chen Y. et al.<sup>[63]</sup> to fabricate N-S/rGO aerogel for the electrode of the SC device. When an IL named EMIMBF<sub>4</sub> was used as an electrolyte, the device showed good energy density and specific capacitance performance. The system displayed high conductivity of 11.5 S cm<sup>-1</sup>. At 0.9 kW kg<sup>-1</sup> of power density, 75 Wh kg<sup>-1</sup> of energy density was produced, and 180.5 F g<sup>-1</sup> of specific capacitance was observed at 1 A g<sup>-1</sup>. When the PD was 15 kW kg<sup>-1</sup>, the device delivered 33 Wh kg<sup>-1</sup> of ED.

Wong et al.<sup>[64]</sup> recently developed a binary mixture of IL to use as an electrolyte for graphene-based SC. Two ILs, i.e., 1-ethyl-3-methylimidazolium bis (trifluoromethyl sulfonyl)imide and butyl trimethylammonium bis (trifluoromethyl sulfonyl)imide, were mixed in different ratios to form binary IL. When it obtained equal proportions of both the ILs, the excellent specific capacitance of 293.1 F g<sup>-1</sup> and high ED of 177 Wh kg<sup>-1</sup>. EMIMBF<sub>4</sub> IL was used as an electrolyte in graphene-based SC.<sup>[65]</sup> The prepared system displays a high specific capacitance of 144.4 F g<sup>-1</sup> at an operating voltage of 3.5 V with an ED of 60.7 Wh kg<sup>-1</sup> and a PD of 10 kW kg<sup>-1</sup>. Table 3 summarizes the utilization of different ILs as electrolytes for graphene and its derivative-based SCs.

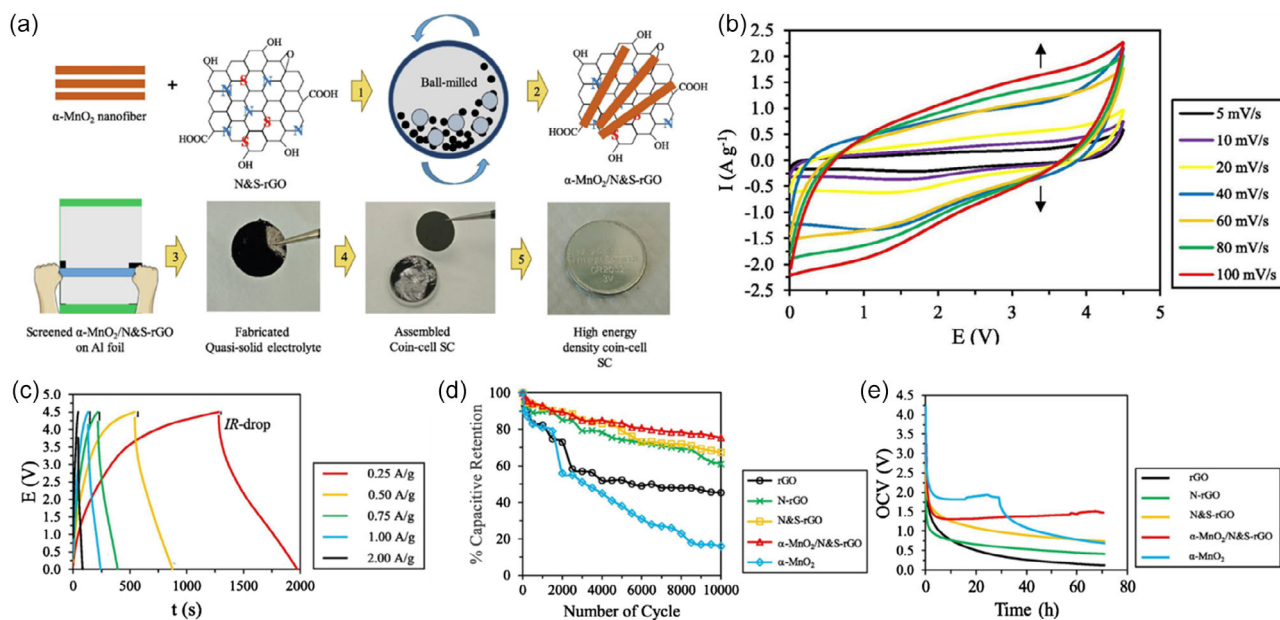


**Figure 7.** a) Graphical representation of synthetic procedure of  $\alpha$ -MnO<sub>2</sub>/N-S/rGO; b,c) CV, GCD curves of  $\alpha$ -MnO<sub>2</sub>/N-S/rGO in IL electrolyte at different scan rates; d) capacitive retention of the prepared SC; e) self-discharge curves w.r.t. discharge time of all electrodes. Reprinted with permission.<sup>[59]</sup> Copyright 2021, Elsevier Ltd.

**Table 3.** Summary of the utilization of ILs as electrolytes for graphene and its derivative-based SCs.

Electrolyte	Electrode	Cell voltage [V]	Surface area	Specific capacitance [F g <sup>-1</sup> ]	Stability	Energy density [Wh kg <sup>-1</sup> ]	Power density	References
1-ethyl-3-methylimidazolium tetrafluoroborate (EMIMBF <sub>4</sub> )	GQDs@ MnO <sub>2</sub>	–	–	208.2	–	82.2	11.6 kW kg <sup>-1</sup>	[58]
EMIMBF <sub>4</sub>	Graphene areogel	–	–	–	–	104-33	944-15 860 kW kg <sup>-1</sup>	[90]
N,N-Diethyl-N-methyl-N-(2-methoxy-ethyl) ammonium bis (trifluoromethyl-sulfonyl)amide	$\alpha$ -MnO <sub>2</sub> /N-S/rGO	4.5	–	165	67% after 10 000 cycles	110	550 kW kg <sup>-1</sup>	[59]
(N-methyl-N-propyl piperidinium bis(fluorosulfonyl)imide (PIP13-FSI) and N-butyl-N-methyl pyrrolidinium bis(fluorosulfonyl)imide)	GO	3.5	1901 m <sup>2</sup> g <sup>-1</sup>	180	–	–	–	[60]
1-butyl-3-methylimidazolium bis(trifluoromethyl sulfonyl) imide ([Bmim][Tf <sub>2</sub> N])	Graphene areogel	–	–	–	–	115-28	946–11 586 kW kg <sup>-1</sup>	[91]
1-butyl-3- methylimidazolium tetrafluoroborate	Graphene	2	–	214	–	33.3	24.7 Wh kg <sup>-1</sup>	[61]
EMIMBF <sub>4</sub>	GO	–	–	196.7	78.3% after 5500 cycles	97.2	0.9 kW kg <sup>-1</sup>	[62]
EMIMBF <sub>4</sub>	rGO-aerogel	–	–	180.5	–	33	15 kW kg <sup>-1</sup>	[63]
1-ethyl-3-methylimidazolium bis(trifluoromethyl sulfonyl)imide and butyl trimethylammonium bis(trifluoromethyl sulfonyl)imide	Graphene based	4.1	–	293.1	–	177	–	[64]
EMIMBF <sub>4</sub>	Graphene based	3.5	–	144.4	–	60.7	10 kW kg <sup>-1</sup>	[65]

### 4.3. Ionic Liquid as Electrolytes for CNTs and CNFs-Based SCs

In recent years, ILs integrated with CNTs have been prepared for application in energy storage/transformation owing to their excellent electronic and electrochemical activity. Among ILs, surface-active 2-ethylhexyl sulfate (EHS) tetraoctylammonium ([N8,8,8,8][EHS]) was used as an electrolyte for multiwalled

CNTs (MWCNTs) based SC.<sup>[66]</sup> The surface-active IL is proven a potential electrolyte as it exhibits decent electrochemical performance with a higher PD of 169 kW kg<sup>-1</sup> and higher ED of 94 Wh kg<sup>-1</sup> at a scan rate of 2 mV s<sup>-1</sup>. The obtained specific capacitance was 169 F g<sup>-1</sup> with a working potential of 4 V. The surface-active IL was fabricated via ion exchange reaction and had an electrical conductivity of 99  $\mu$ S cm<sup>-1</sup> at 373 K and stable

up to 530 K temperature as observed from the thermal gravimetric analysis. In addition to this, Jain and Antzutkin<sup>[67]</sup> again prepared surface-active IL [EHS][1-methyl-3-hexylimidazolium] through metathesis reactions which were utilized as an electrolyte for MWCNT-based SC. The observed ionic conductivity of the system at 298 and 373 K was  $73.19 \mu\text{S cm}^{-1}$  and  $1.62 \text{ mS cm}^{-1}$ , respectively. Further, at 298 K, a specific capacitance of  $148 \text{ F g}^{-1}$  and ED of  $82 \text{ Wh kg}^{-1}$  was obtained, and at 373 K, the obtained specific capacitance was  $290 \text{ F g}^{-1}$  with an ED of  $161 \text{ Wh kg}^{-1}$ . Li M. et al.<sup>[68]</sup> fabricated  $\alpha\text{-MnO}_2$  on CF-modified CNT ( $\alpha\text{-MnO}_2\text{@CNTs/CNFs}$ ), which was used as positive and negative electrodes for SC. The electrode was prepared by chemical vapor deposition followed by the hydrothermal method as described in **Figure 8a** along with b unit cell and c crystal structure of  $\alpha\text{-MnO}_2$ , and EMIMBF<sub>4</sub> was utilized as electrolyte. At an operating voltage of 4 V, CV curves, as shown in **Figure 8d**, confirmed that the material showed pseudocapacitive property even at a sweep rate of  $2400 \text{ mV s}^{-1}$  and exhibited a specific capacitance of  $78.2 \text{ F g}^{-1}$ . GCD curves in **Figure 8e** show that the device displays an energy density of  $160.4 \text{ Wh kg}^{-1}$  with a power density of  $2000 \text{ W kg}^{-1}$ . Furthermore, the machine had a capacitive retention of 78.95% after 5000 runs.

By single-step neutralization method, nonfluorinated IL [P4444][HFuA] was prepared by a team of researchers<sup>[46b]</sup> to utilize as an electrolyte in MWCNTs/AC electrode-based SC. Electrochemical measurements revealed that the device had a maximum specific capacitance of  $174.2 \text{ F g}^{-1}$  with a scan rate of  $5 \text{ mV s}^{-1}$  at  $100^\circ\text{C}$ . CV study displayed that the device shows a retention capacitance of 90% at  $60^\circ\text{C}$ . Noremberg et al.<sup>[69]</sup>

utilized 1-n-butyl-3-methylimidazolium bis(trifluoromethane sulfonyl)imide as an electrolyte in cellulose/MWCNTs-based SC. The surface area of the as-prepared material was  $74.4 \text{ m}^2 \text{ g}^{-1}$ , and the system had a specific capacitance of  $34.37 \text{ F g}^{-1}$  with a retaining capacitance of 97.9% after 5000 runs. Other researchers reported the effect of the size of the diameters of single-walled CNTs (SWCNTs) on the performance of IL-based SC.<sup>[4a]</sup> Triethyl(2-methoxyethyl) phosphonium bis(trifluoromethyl sulfonyl)imide was utilized as an electrolyte, and electrochemical performance was measured up to  $150^\circ\text{C}$ . The capacitance value surges from 15.8 (room temperature) to 27.5 ( $150^\circ\text{C}$ ) on a current density of  $5 \text{ mA g}^{-1}$  when SWCNT of 1 nm was used. The SWCNTs having a diameter of more than 1 nm did not significantly affect the device's capacitance with increasing temperature.

1-Butyl-3-methylimidazolium bis (trifluoromethyl sulfonyl) imide was employed as electrolytes for SC based on MWCNTs electrode modified with the same IL and hydrogen exfoliated graphene. The role of MWCNTs was a bridge and spacer for the transfer of electrons between graphene sheets. The obtained material had a larger exterior area of  $166.47 \text{ m}^2 \text{ g}^{-1}$  and a pore volume of  $4.429 \text{ cm}^3 \text{ g}^{-1}$ , corresponding to a pore size of 3.54 nm. The larger pore size of nanocomposite compared to IL results in the enhancement of specific capacitance due to better accessibility of electrolytes. The device displayed a higher specific capacitance of  $201 \text{ F g}^{-1}$  with an ED of  $171 \text{ Wh kg}^{-1}$  and a PD of  $148 \text{ kW kg}^{-1}$  at an operating voltage of 3.5 V.<sup>[70]</sup> Tamilarasan and Ramaprabhu synthesized MWCNT-based electrode modified with 1-butyl-3-methylimidazolium bis(trifluoromethyl sulfonyl)imide via the Hummers method for SC device.<sup>[71]</sup> The authors related the

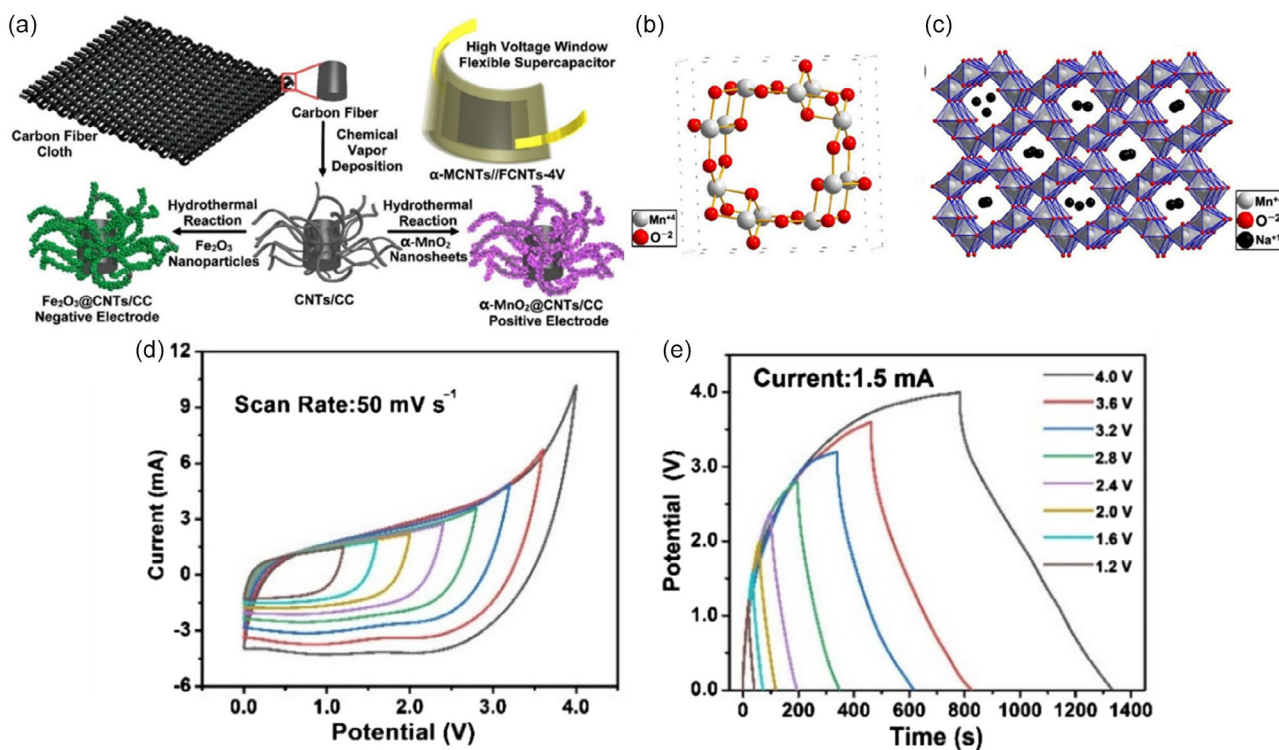


**Figure 8.** a–c) Graphic illustration of the synthetic procedure of  $\alpha\text{-MnO}_2\text{@CNTs/CNFs}$ , unit cell and crystal structure of  $\alpha\text{-MnO}_2$ ; d,e) CV, GCD curves of  $\alpha\text{-MnO}_2\text{@CNTs/CNFs}$ . Reprinted with permission.<sup>[68]</sup> Copyright 2022, MDPI.

performance of IL-based material with bare MWCNTs and observed that IL enhances the device's performance by 85%. The observed specific capacitance was  $242 \text{ F g}^{-1}$  at a current density of  $2 \text{ A g}^{-1}$  and showed a retention capacitance of 98% after 1000 cycles. Observed maximum ED and PDs were  $107.06 \text{ Wh kg}^{-1}$  and  $8.79 \text{ kW kg}^{-1}$ . [EMIM] bis(trifluoromethyl sulfonyl) imide-based gel electrolyte was utilized in CNT-based SC.<sup>[72]</sup> At a current density of  $2 \text{ A g}^{-1}$ , the SC exhibits  $135 \text{ F g}^{-1}$  of specific capacitance,  $41 \text{ Wh kg}^{-1}$  ED, and  $164 \text{ kW kg}^{-1}$  PD.

[EMIM] bis(trifluoromethyl sulfonyl)imide was utilized as an electrolyte in CNF-based SC by Kim et al.,<sup>[73]</sup> which results in an excellent energy density of  $246 \text{ Wh kg}^{-1}$  by a specific capacitance of  $161 \text{ F g}^{-1}$ . The surface area of the CNF-based electrode was  $1624 \text{ m}^2 \text{ g}^{-1}$  with a pore size of  $0.831 \text{ nm}$ . This larger surface area helped in achieving outstanding electrochemical performance. Again, [EMIM] bis(trifluoromethyl sulfonyl) imide-based

ionogel was used as an electrolyte for CNF-based SC. The surface area of the electrode was  $2282 \text{ m}^2 \text{ g}^{-1}$ , which results in higher interaction of the surface of the electrode with the electrolyte and improves the device's electrochemical performance. The device's energy density was  $65 \text{ Wh kg}^{-1}$  with a gravimetric capacitance of  $153 \text{ F g}^{-1}$  at a cell voltage of  $3.5 \text{ V}$ . The device is highly stable and showed retention capacitance of 96% after 20 thousand cycles.<sup>[74]</sup> Sun Y. et al.<sup>[75]</sup> prepared porous CNF-based material by electro-spinning technique to use it as an electrode and EMIMBF<sub>4</sub> as an electrolyte in SC. The electrode modified with as-synthesized material had a surface area of  $1177 \text{ m}^2 \text{ g}^{-1}$  and a specific capacitance of  $101.9 \text{ F g}^{-1}$  with ED and PD of  $60.1 \text{ Wh kg}^{-1}$  and  $35 \text{ kW kg}^{-1}$ , correspondingly. The trial of the PCF-*x* is sequentially shown within **Figure 9a**. Figure 9b illustrates CV arcs of PCF-1.0//PCF-1.0 SC from 10 to  $200 \text{ mV s}^{-1}$  in EMIMBF<sub>4</sub> media. All CV arcs are comparable at sweep rates

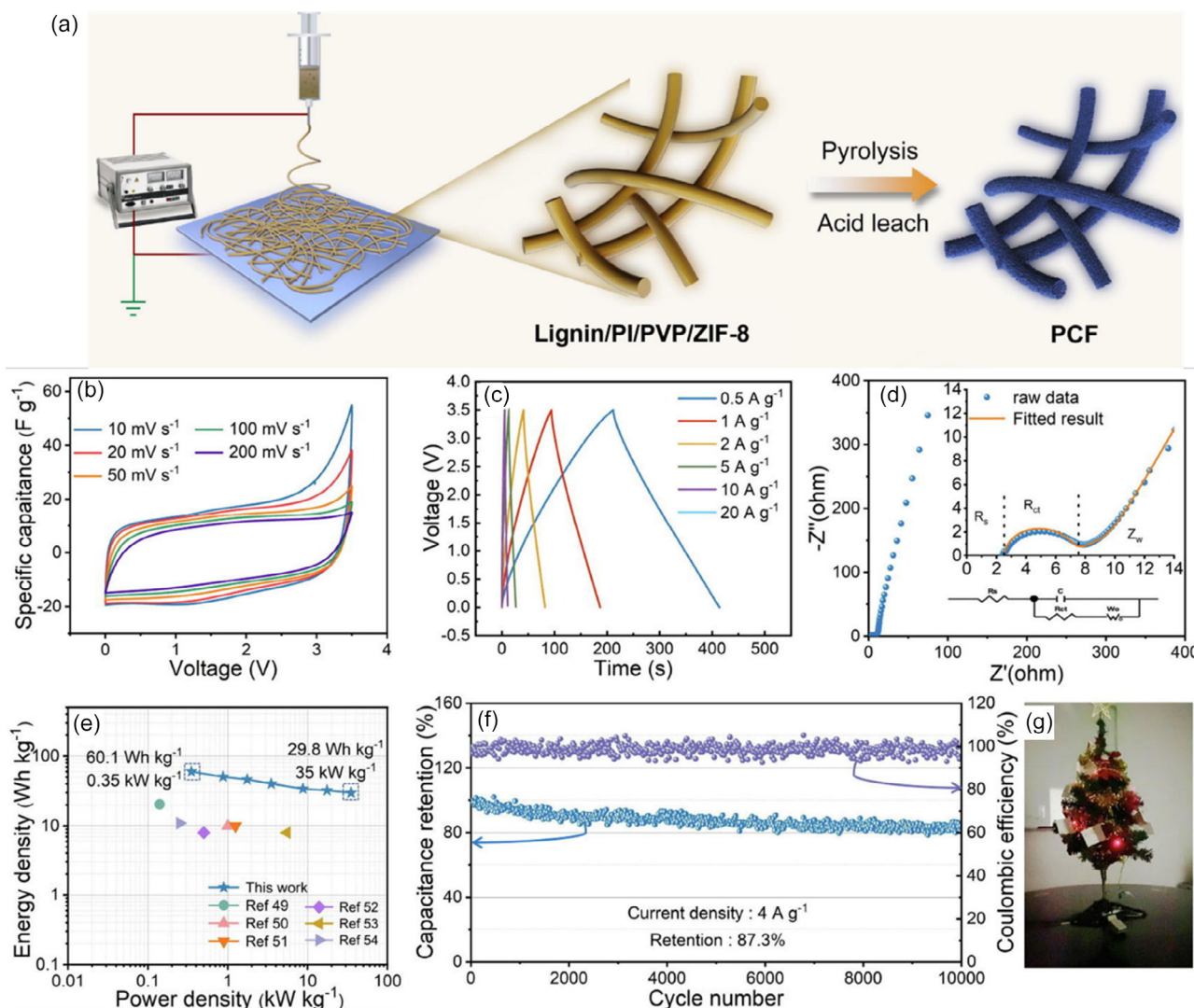


**Figure 9.** a) Diagram design of the formulating of the PCF-*x* model. SC routine of the PCF-1.0 electrode utilizing IL of EMIMBF<sub>4</sub>. b) CV graphs. c) GCD arcs. d) Nyquist designs. Inserts demonstrate high-frequency area and tailored equivalent circuit style. e) Ragone schemes of a symmetrical capacitor based upon diverse carbon substances. f) Long-standing cycling recital of the PCF-1.0 electrode at  $4 \text{ A g}^{-1}$ . g) Picture of LED bulbs power driven by one device. Reprinted with permission.<sup>[75]</sup> Copyright 2021, Elsevier Ltd.

varying as of 10–200 mV s<sup>-1</sup>. Similarly, the GCD arcs demonstrate an alike isosceles triangle-shape form, displaying better reversibility and EDLC performance (Figure 9c). Particularly, the apparatus also shows a suitable capacitance about 101.9 F g<sup>-1</sup> and maintains 61% of its preliminary capacitance once raised the current density after 0.5 A to 20 A g<sup>-1</sup>. To show the kinetics of the PCF-1.0//PCF-1.0 machine, EIS analyzed occurrences 0.01 Hz to 100 kHz (Figure 9d). Lower resistance values of  $R_s$  (2.54 Ω),  $R_{ct}$  (4.31 Ω), and Warburg constant ( $Z_w$ , 7 Ω) intended for the PCF-1.0 appliance may be accredited toward the favorable configuration of as-obtained PCF-1.0. Similarly, the PCF-1.0-based apparatus provides the most increased ED ( $E_{max}$ ) of 60.1 Wh kg<sup>-1</sup> on a PD of 0.35 kW kg<sup>-1</sup>, more elevated compared to some documented

carbon-based apparatuses (Figure 9e). The electrochemical stability with better retaining (87.3%) for 10 000 runs and nearly 100% Coulombic efficiency also shows the high reversibility and durable electrochemical performance of PCF-1.0-based SC. It is crucial noting that after cycling trials, the apparatus may still show gratifying EDLC behavior backed via CV and GCD data (Figure 9f), which may hold around 80% capacitance retaining of the primary behavior. Additionally, the formed SC based upon the IL approach immediately operated as the power origin to light parallel LED lights (3 V) intersection upon a Christmas tree, showing the practical implementation of the appliance (Figure 9g).

**Table 4** summarizes the utilization of ILs as electrolytes for CNTs, CNFs, and other carbon-based SCs.

**Table 4.** Summary of the utilization of ILs as electrolytes for CNTs, CNFs, and other carbon-based SCs.

Electrolyte	Electrode	Cell voltage [V]	Surface area [m <sup>2</sup> g <sup>-1</sup> ]	Specific capacitance	Stability	Energy density	Power density	References
[N8,8,8][EHS]	MWCNT	4	–	169 F g <sup>-1</sup>	–	94 Wh kg <sup>-1</sup>	169 kW kg <sup>-1</sup>	[66]
EMIMBF <sub>4</sub>	α-MnO <sub>2</sub> @CNTs/CNFs	4	–	78.2 F g <sup>-1</sup>	78.95% after 5000 cycles	160.4 Wh kg <sup>-1</sup>	2000 W kg <sup>-1</sup>	[68]
[EHS][1-methyl-3-hexylimidazolium]	MWCNT	–	–	290 F g <sup>-1</sup>	–	161 Wh kg <sup>-1</sup>	–	[67]
1-n-butyl-3-methylimidazolium bis(trifluoromethane sulfonyl)imide	MWCNT	–	74.4	34.37 F g <sup>-1</sup>	97.9% after 5000 cycles	–	–	[69]
1-butyl-3-methylimidazolium bis(trifluoromethyl sulfonyl) imide	MWCNTs/hydrogen-exfoliated graphene/1-butyl-3-methylimidazolium bis(trifluoromethyl sulfonyl) imide	3.5	166.47	201 F g <sup>-1</sup>	98% after 1000 cycles	171 Wh kg <sup>-1</sup>	148.43 kW kg <sup>-1</sup>	[70]
1-butyl-3-methylimidazolium bis(trifluoromethyl sulfonyl)imide	MWCNTs	–	–	242 F g <sup>-1</sup>	98% after 1000 cycles	107.06 Wh kg <sup>-1</sup>	8.79 kW kg <sup>-1</sup>	[71]
[EMIM] bis(trifluoromethyl sulfonyl)imide	CNF	3.5	1624	161 F g <sup>-1</sup>	–	246 Wh kg <sup>-1</sup>	–	[73]
N-butyl N-methyl pyrrolidinium bis(trifluoromethanesulfonyl)imide	Lignin-derived CNF	3.5	2770	87 F g <sup>-1</sup>	98% after 1000 cycles	38 Wh kg <sup>-1</sup>	1666 W kg <sup>-1</sup>	[92]
EMIMBF <sub>4</sub>	CNT/stainless steel core-sheath yarn	–	–	329.13 F g <sup>-1</sup>	–	6.67 × 10 <sup>-2</sup> Wh cm <sup>-3</sup>	8.89 W cm <sup>-3</sup>	[93]
[EMIM] bis(trifluoromethyl sulfonyl)imide	CNF	3.5	2282	153 F g <sup>-1</sup>	96% after 20 000 cycles	65 Wh kg <sup>-1</sup>	–	[74]
EMIMBF <sub>4</sub>	CNF	3.5	1177	101.9 F g <sup>-1</sup>	87.3% after 10 000 cycles	60.1 Wh kg <sup>-1</sup>	35 kW kg <sup>-1</sup>	[75]
[EMIM] bis(trifluoromethyl sulfonyl)imide	CNF	3.5	2282	144 F g <sup>-1</sup>	–	61 Wh kg <sup>-1</sup>	–	[94]
[EDMF]BF <sub>4</sub>	Glassy carbon	2.7	2073	165 F g <sup>-1</sup>	Stable up to 5000 cycles	489.5 kWh kg <sup>-1</sup>	–	[95]
Imidazolium type	N-doped porous carbon	2.3	1310	333 F g <sup>-1</sup>	53.5 % after 10 000 cycles	48.3 Wh kg <sup>-1</sup>	1.75 kW kg <sup>-1</sup>	[96]
EMIMBF <sub>4</sub>	Cu-Co selenide nanowires modified CNFs	–	195.652	28.63 F g <sup>-1</sup>	77.3%	191.6 mWh kg <sup>-1</sup>	36.65 W kg <sup>-1</sup>	[97]
EMIMBF <sub>4</sub>	Porous carbon	–	2807	218 F g <sup>-1</sup>	88% after 10 000 cycles	93 Wh kg <sup>-1</sup>	1.75 kW kg <sup>-1</sup>	[98]
EMIMBF <sub>4</sub> gel electrolyte	N, O doped carbon hydrangeas	3.5	2212	218 F g <sup>-1</sup>	90%	101.2 Wh kg <sup>-1</sup>	875 W kg <sup>-1</sup>	[48]
EMIM-thiocyanate	Porous carbon	–	879.69	294 F g <sup>-1</sup>	–	–	–	[99]
1-Methyl-1-propylpyrrolidinium bis(trifluoromethyl sulfonyl)imide	Diamond-coated Si-wires	4	–	105 μF cm <sup>-2</sup>	–	84 μJ cm <sup>-2</sup>	0.94 mW cm <sup>-2</sup>	[100]
EMIBF <sub>4</sub>	Porous carbon	–	–	166 F g <sup>-1</sup>	93.1%	59 Wh kg <sup>-1</sup>	59 kW kg <sup>-1</sup>	[101]

## 5. Importance of IL-Based Materials from Other Materials

Physical properties such as absorption/desorption, surface area, and coupling between electrode and electrolyte are involved in the performance of SCs. Capacitance of SCs depends on the interaction of electrode and electrolyte, and the energy density of the system is dependent on potential window. Larger potential window results in higher energy densities of the system.<sup>[45]</sup> Further, wide temperature range is required for the devices specially in portable devices.

ILs are adequate nominees for SCs, specifically that functioning based upon the double-layer charging, for two reasons: the initial task of the media is to provide charge species at the electrode/electrolyte boundary rather than diffusion of specific electroactive types, vast and the steady potential range of ILs ensures better EDs even more significant than those of organic media. Additionally, the practical applications of ILs as solvent-free electrolyte-based procedures for elemental analyses to understand the essence of electrode/electrolyte interface in SCs. Remark that the complexity of ILs is owing to the originality of these electrolytes compared with conventional electrolytes. The developing curiousness in ILs was owing to the practical possibility, and inappropriately, there are only an inadequate number of essential analysis (primarily theoretical) concentrating upon the electrode/electrolyte edge of SCs in ILs: 1) ILs provide stable broad potential window that surely provides high-energy densities to the system.<sup>[76]</sup> Also, ILs are thermally more stable which ensures elevated temperature range to SC systems. Hence, ILs are considered as superior electrolytes over other conventional electrolytes for energy storage devices.

For instance, Oyedotun et al.<sup>[77]</sup> fabricated carbon nanofibers to be utilized as electrode material in SCs. The authors studied the effect of electrolytes on the system's performance and observed a wider potential window of nearly 3 V for IL electrolytes compared to aqueous electrolytes Na<sub>2</sub>SO<sub>4</sub> and KOH, which showed a potential window of 0.8 V. Due to this broader potential range, the device obtained a high energy density of 24.0 Wh kg<sup>-1</sup> at a power density of 750.3 W kg<sup>-1</sup>, while energy densities for aqueous electrolytes Na<sub>2</sub>SO<sub>4</sub> and KOH were 3.3 and 8.1 Wh kg<sup>-1</sup> at power densities of 200 and 177.4 W kg<sup>-1</sup>, respectively.

In addition to this, controlled growth of carbon materials can be achieved by utilizing ILs as reaction media, which helps in avoiding cross-linking of neighboring carbons, so minimizes the agglomeration. The porosity of carbons can also be improved by utilization of ILs as reaction media.<sup>[78]</sup> Conventional solvents/catalysts are not recycled frequently; however, recycling of ILs is easy particularly in case of two-phase system.<sup>[79]</sup> Other important feature of ILs which make them superior solvent/catalyst over other conventional materials is their high durability and high degree of conversion without much loss of IL solvent/catalyst.<sup>[80]</sup>

## 6. Conclusion and Future Prospects

The significant advancement in energy storage devices is motivated by the emerging expectations toward sustainability in the energy technology field caused by the ever-growing energy crisis globally. SCs attract tremendous focus for mobile power supply

and instant storage of energy. The performance of SCs relies on physiochemical and dynamic interactions at the interface of the electrolyte and the electrode. Carbon-based materials are widely used as SCs electrodes. ILs anticipate the development of advanced SCs with high energy owing to their outstanding characteristics, which are illustrated in the sections mentioned are. ILs are versatile in SCs as ideal precursors and media for generating carbon-based materials and as electrolytes for carbon-based SCs.

There are numerous applications of IL-based carbons. Nitrogen-doped carbons are broadly employed as electrode substances within fuel cells and SCs. Heterogeneous catalysis, for example, selective oxidation, is another primary application of these carbons. However, the prospect of ILs in carbon substances still needs to be wholly manipulated. It must consider cost and sustainability cases for practical applications, which could impede the commercial-scale preparation of carbons via the direct carbonization of ILs.

It can achieve the requirement of sustainable and green procedures for producing carbon-based materials due to the versatile structure of ILs, tuned porosity, and their recycling property. Nevertheless, the exploitation of ILs in carbon-based materials is still needed, and for large-scale production of carbons, we must consider the issue of sustainability and cost. For the fabrication of functionalized carbon electrodes, we must take the direct pyrolysis of ILs method into account, where ILs act as dopants, template, and source of carbon. Multiple coupling of anions and cations can ameliorate the performance of the electrode; therefore, we must understand the correlation of structure and the property of IL and carbon material. In addition, some efforts must be attempted to build an all-in-one IL-derived SC device where the single system consists of IL-derived electrodes and electrolytes. For the future growth of this domain, the coating/captivity of ILs on/in affordable bulk supports is advantageous. Additionally, somewhat inexpensive ILs, such as those emanating from biomass, are also attractive for carbon-based materials preparation.

## Acknowledgements

The authors acknowledge the support from the Department of Chemistry and Research & Development Cell of Maharishi Markandeshwar (Deemed to be University), Mullana, Ambala, Haryana, India.

## Conflict of Interest

The authors declare no conflict of interest.

## Keywords

carbon nanotubes, carbon-based materials, ionic liquids, nitrogen-doped carbons, supercapacitors

Received: February 8, 2023

Revised: April 5, 2023

Published online:

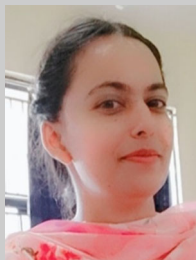
- [1] A. A. Hor, N. Yadav, S. A. Hashmi, *J. Energy Storage* **2022**, *47*, 103608.
- [2] L. Miao, Z. Song, D. Zhu, L. Li, L. Gan, M. Liu, *Mater. Adv.* **2020**, *1*, 945.
- [3] a) M. V. Lebedeva, P. M. Yeletsky, A. B. Ayupov, A. N. Kuznetsov, E. N. Gribov, V. N. Parmon, *Catal. Ind.* **2018**, *10*, 173; b) M. Karnan, K. Hari Prakash, S. Badhulika, *J. Energy Storage* **2022**, *53*, 105189; c) S. S. Siwal, Q. Zhang, N. Devi, K. V. Thakur, *Polymers* **2020**, *12*, 505.
- [4] a) A. Al-zubaidi, N. Asai, Y. Ishii, S. Kawasaki, *RSC Adv.* **2020**, *10*, 41209; b) X. Luo, Q. Yang, Y. Dong, X. Huang, D. Kong, B. Wang, H. Liu, Z. Xiao, L. Zhi, *J. Mater. Chem. A* **2020**, *8*, 17558; c) S. S. Siwal, A. K. Saini, S. Rarotra, Q. Zhang, V. K. Thakur, *J. Nanostruct. Chem.* **2021**, *11*, 93.
- [5] a) M. A. Garakani, S. Bellani, V. Pellegrini, R. Oropesa-Nuñez, A. E. D. R. Castillo, S. Abouali, L. Najafi, B. Martín-García, A. Ansaldo, P. Bondavalli, C. Demirci, V. Romano, E. Mantero, L. Marasco, M. Prato, G. Bracciale, F. Bonaccorso, *Energy Storage Mat.* **2021**, *34*, 1; b) E. Payami, A. Aghaiepour, K. Rahimpour, R. Mohammadi, R. Teimuri-Mofrad, *J. Alloys Compd.* **2020**, *829*, 154485.
- [6] a) X. Zhou, Y. Wang, C. Gong, B. Liu, G. Wei, *Chem. Eng. J.* **2020**, *402*, 126189; b) B. Jeon, T. Ha, D. Y. Lee, M.-S. Choi, S. W. Lee, K.-H. Jung, *Polymers* **2020**, *12*, 1851.
- [7] a) Y. Gao, S. Zheng, H. Fu, J. Ma, X. Xu, L. Guan, H. Wu, Z.-S. Wu, *Carbon* **2020**, *168*, 701; b) J. Yan, L. Miao, H. Duan, D. Zhu, Y. Lv, W. Xiong, L. Li, L. Gan, M. Liu, *Electrochim. Acta* **2020**, *358*, 136899; c) S. Karamveer, V. K. Thakur, S. S. Siwal, *Mater. Today Proc.* **2022**, *56*, 9.
- [8] a) N. Zdolšek, R. P. Rocha, J. Krstić, T. Trtić-Petrović, B. Šljukić, J. L. Figueiredo, M. J. Vujković, *Electrochim. Acta* **2019**, *298*, 541; b) E. Frackowiak, *Phys. Chem. Chem. Phys.* **2007**, *9*, 1774.
- [9] a) Z.-L. Xie, D. S. Su, *Eur. J. Inorg. Chem.* **2015**, *2015*, 1137; b) K. Sheoran, H. Kaur, S. S. Siwal, A. K. Saini, D.-V. N. Vo, V. K. Thakur, *Chemosphere* **2022**, *299*, 134364.
- [10] a) J. P. Paraknowitsch, Y. Zhang, A. Thomas, *J. Mater. Chem.* **2011**, *21*, 15537; b) K. Beniwal, H. Kaur, A. K. Saini, S. S. Siwal, *Nanofabrication* **2022**, *7*, 174.
- [11] a) X. Zhang, D. Su, L. Xiao, W. Wu, *J. CO<sub>2</sub> Util.* **2017**, *17*, 37; b) Z.-L. Xie, R. J. White, J. Weber, A. Taubert, M. M. Titirici, *J. Mater. Chem.* **2011**, *21*, 7434.
- [12] P. F. R. Ortega, G. A. d. Santos Jr., J. P. C. Trigueiro, G. G. Silva, N. Quintanal, C. Blanco, R. L. Lavall, R. Santamaría, *J. Phys. Chem. C* **2020**, *124*, 15818.
- [13] J. Gong, H. Lin, M. Antonietti, J. Yuan, *J. Mater. Chem. A* **2016**, *4*, 7313.
- [14] K. Mishra, N. Devi, S. S. Siwal, Q. Zhang, W. F. Alsanie, F. Scarpa, V. K. Thakur, *Adv. Sci.* **2022**, *9*, 2202187.
- [15] a) Z. Cai, R. Chen, H. Zhang, F. Li, J. Long, L. Jiang, X. Li, *Green Chem.* **2021**, *23*, 10116; b) K. Mishra, V. Kumar Thakur, S. Singh Siwal, *Mater. Today Proc.* **2022**, *56*, 107; c) M. Watanabe, M. L. Thomas, S. Zhang, K. Ueno, T. Yasuda, K. Dokko, *Chem. Rev.* **2017**, *117*, 7190.
- [16] a) N. Devi, S. S. Siwal, *Nanofabrication* **2022**, *7*, 165; b) S. S. Siwal, W. Yang, Q. Zhang, *J. Energy Chem.* **2020**, *51*, 113; c) J. Zeng, L. Chen, S. Siwal, Q. Zhang, *Sustainable Energy Fuels* **2019**, *3*, 1957–1965.
- [17] J. Zeng, J. Liu, S. S. Siwal, W. Yang, X. Fu, Q. Zhang, *Appl. Surf. Sci.* **2019**, *491*, 570.
- [18] P. Walden, *Bull. Acad. Imper. Sci. (St. Petersburg)* **1914**, *1800*, 1800.
- [19] C. Cruz, A. Ciach, *Molecules* **2021**, *26*, 3668.
- [20] S. Shahzad, A. Shah, E. Kowsari, F. J. Iftikhar, A. Nawab, B. Piro, M. S. Akhter, U. A. Rana, Y. Zou, *Global Challenges* **2019**, *3*, 1800023.
- [21] a) H. Tokuda, K. Hayamizu, K. Ishii, M. A. B. H. Susan, M. Watanabe, *J. Phys. Chem. B* **2005**, *109*, 6103; b) H. Kaur, V. K. Thakur, S. S. Siwal, *Mater. Today Proc.* **2022**, *56*, 112.
- [22] M. P. S. Mousavi, B. E. Wilson, S. Kashefolgheta, E. L. Anderson, S. He, P. Bühlmann, A. Stein, *ACS Appl. Mater. Interfaces* **2016**, *8*, 3396.
- [23] V. Ruiz, T. Huynh, S. R. Sivakkumar, A. G. Pandolfo, *RSC Adv.* **2012**, *2*, 5591.
- [24] L. Yu, G. Z. Chen, *Front. Chem.* **2019**, *7*, <https://doi.org/10.3389/fchem.2019.00272>.
- [25] a) H. Kaur, S. S. Siwal, G. Chauhan, A. K. Saini, A. Kumari, V. K. Thakur, *Chemosphere* **2022**, *304*, 135182; b) S. S. Siwal, H. Kaur, A. K. Saini, V. K. Thakur, *Adv. Energy Sustainable Res.* **2022**, *3*, 2200062.
- [26] a) Z.-Y. Jin, A.-H. Lu, Y.-Y. Xu, J.-T. Zhang, W.-C. Li, *Adv. Mater.* **2014**, *26*, 3700; b) L. L. Zhang, X. S. Zhao, *Chem. Soc. Rev.* **2009**, *38*, 2520.
- [27] a) Z. Song, L. Miao, Y. Lv, L. Gan, M. Liu, *J. Mater. Chem. A* **2023**, <https://doi.org/10.1039/D2TA09258A>.
- [28] a) Y. Zhang, J. Wang, G. Shen, J. Duan, S. Zhang, *Front. Chem.* **2020**, *8*, <https://doi.org/10.3389/fchem.2020.00196>; b) D. S. Su, S. Perathoner, G. Centi, *Chem. Rev.* **2013**, *113*, 5782.
- [29] M. Baccour, N. Louvain, J. G. Alauzun, L. Stievano, P. H. Mutin, B. Boury, L. Monconduit, N. Brun, *J. Power Sources* **2020**, *474*, 228575.
- [30] S. Zhang, K. Dokko, M. Watanabe, *Chem. Mater.* **2014**, *26*, 2915.
- [31] X. Fu, A. Chen, Y. Yu, S. Hou, L. Liu, *Chem. Asian J.* **2019**, *14*, 634.
- [32] G. Wang, Z. Ling, C. Li, Q. Dong, B. Qian, J. Qiu, *Electrochem. Commun.* **2013**, *31*, 31.
- [33] B. Qiu, C. Pan, W. Qian, Y. Peng, L. Qiu, F. Yan, *J. Mater. Chem. A* **2013**, *1*, 6373.
- [34] Z. Li, Q. Xu, L. Zhang, X. Wang, F. He, J. Cheng, H. Xie, *Sustain. Energy Fuels* **2020**, *4*, 3418.
- [35] H. Zhou, S. Wu, H. Wang, Y. Li, X. Liu, Y. Zhou, *J. Hazard. Mater.* **2021**, *402*, 124023.
- [36] H. Zhou, Y. Zhou, L. Li, Y. Li, X. Liu, P. Zhao, B. Gao, *ACS Sustainable Chem. Eng.* **2019**, *7*, 9281.
- [37] C. Liu, Y. Hou, Y. Li, H. Xiao, *J. Colloid Interface Sci.* **2022**, *614*, 566.
- [38] Q. Xu, X. Wang, J. Cheng, L. Zhang, F. He, H. Xie, *RSC Adv.* **2020**, *10*, 36504.
- [39] L. Miao, D. Zhu, M. Liu, H. Duan, Z. Wang, Y. Lv, W. Xiong, Q. Zhu, L. Li, X. Chai, L. Gan, *Chem. Eng. J.* **2018**, *347*, 233.
- [40] a) F. Béguin, V. Presser, A. Balducci, E. Frackowiak, *Adv. Mater.* **2014**, *26*, 2219; b) B. Pal, S. Yang, S. Ramesh, V. Thangadurai, R. Jose, *Nanoscale Adv.* **2019**, *1*, 3807.
- [41] T. Ouyang, T. Zhang, H. Wang, F. Yang, J. Yan, K. Zhu, K. Ye, G. Wang, L. Zhou, K. Cheng, D. Cao, *Chem. Eng. J.* **2018**, *352*, 459.
- [42] J. Yan, D. Zhu, Y. Lv, W. Xiong, M. Liu, L. Gan, *Chin. Chem. Lett.* **2020**, *31*, 579.
- [43] P. M. Yeletsky, M. V. Lebedeva, V. A. Yakovlev, *J. Energy Storage* **2022**, *50*, 104225.
- [44] a) L. Miao, Z. Song, D. Zhu, L. Li, L. Gan, M. Liu, *Energy Fuels* **2021**, *35*, 8443; b) A. Mishra, N. P. Shetti, S. Basu, K. R. Reddy, T. M. Aminabhavi, in *Green Sustainable Process for Chemical and Environmental Engineering and Science* (Eds: A. M. Asiri Inamuddin, S. Kanchi) Elsevier **2020**, ISBN: 9780128173862.
- [45] S. Pan, M. Yao, J. Zhang, B. Li, C. Xing, X. Song, P. Su, H. Zhang, *Front. Chem.* **2020**, *8*, 14329.
- [46] a) J. Watson, G. Castro, *J. Mater. Sci. Mater. Electron.* **2015**, *26*, 9226; b) I. A. Khan, Y.-L. Wang, F. U. Shah, *J. Energy Chem.* **2022**, *69*, 174.
- [47] a) X. Wang, H. Zhou, E. Sheridan, J. C. Walmsley, D. Ren, D. Chen, *Energy Environ. Sci.* **2016**, *9*, 232; b) C. Lian, D.-e. Jiang, H. Liu, J. Wu, *J. Phys. Chem. C* **2016**, *120*, 8704.
- [48] Z. Song, H. Duan, L. Miao, L. Ruhlmann, Y. Lv, W. Xiong, D. Zhu, L. Li, L. Gan, M. Liu, *Carbon* **2020**, *168*, 499.



- [49] J. Kong, L. Liu, X. Li, Y. Yang, X. Chen, Y. Fei, L. Xu, Z. Chen, *J. Mol. Liq.* **2022**, 365, 120114.
- [50] S. Fleischmann, M. Widmaier, A. Schreiber, H. Shim, F. M. Stiemke, T. J. S. Schubert, V. Presser, *Energy Storage Mater.* **2019**, 16, 391.
- [51] a) N. Sudhan, K. Subramani, M. Karnan, N. Ilayaraja, M. Sathish, *Energy Fuels* **2017**, 31, 977; b) J. Hou, C. Cao, F. Idrees, X. Ma, *ACS Nano* **2015**, 9, 2556.
- [52] M. K. Sahoo, G. R. Rao, *Nanoscale Adv.* **2021**, 3, 5417.
- [53] Hurilechaoketu, J. Wang, C. Cui, W. Qian, *Carbon* **2019**, 154, 1.
- [54] S. Pilathottathil, K. K. Thasneema, M. Shahin Thayyil, M. P. Pillai, C. V. Niveditha, *Mater. Res. Express* **2017**, 4, 075503.
- [55] M. Anouti, E. Couadou, L. Timperman, H. Galiano, *Electrochim. Acta* **2012**, 64, 110.
- [56] L. Timperman, A. Vigeant, M. Anouti, *Electrochim. Acta* **2015**, 155, 164.
- [57] a) L. Jiang, L. Sheng, C. Long, T. Wei, Z. Fan, *Adv. Energy Mater.* **2015**, 5, 1500771; b) X. Liu, Y. Zheng, X. Wang, *Chem. Eur. J.* **2015**, 21, 10408.
- [58] H. Zhu, L. Li, M. Shi, P. Xiao, Y. Liu, X. Yan, *Chem. Eng. J.* **2022**, 437, 135301.
- [59] C. Poochai, C. Sriprachubwong, J. Sotipinta, J. Lohitkarn, P. Pasakon, V. Primpray, N. Maeboonruan, T. Lomas, A. Wisitsoraat, A. Tuantranont, *J. Colloid Interface Sci.* **2021**, 583, 734.
- [60] W.-Y. Tsai, R. Lin, S. Murali, L. Li Zhang, J. K. McDonough, R. S. Ruoff, P.-L. Taberna, Y. Gogotsi, P. Simon, *Nano Energy* **2013**, 2, 403.
- [61] A. M. Obeidat, V. Luthra, A. C. Rastogi, *J. Solid State Electrochem.* **2019**, 23, 1667.
- [62] Y. Chen, Y. Jiang, Z. Liu, L. Yang, Q. Du, K. Zhuo, *Electrochim. Acta* **2021**, 366, 137414.
- [63] Y. Chen, L. Sun, Z. Liu, Y. Jiang, K. Zhuo, *Mater. Chem. Phys.* **2019**, 238, 121932.
- [64] S. I. Wong, H. Lin, T. Ma, J. Sunarso, B. T. Wong, B. Jia, *Mater. Rep. Energy* **2022**, 2, 100093.
- [65] Z. Lei, Z. Liu, H. Wang, X. Sun, L. Lu, X. S. Zhao, *J. Mater. Chem. A* **2013**, 1, 2313.
- [66] P. Jain, O. N. Antzutkin, *ACS Appl. Energy Mater.* **2021**, 4, 7775.
- [67] P. Jain, O. N. Antzutkin, *J. Ionic Liq.* **2022**, 2, 100034.
- [68] M. Li, K. Zhu, H. Zhao, Z. Meng, C. Wang, P. K. Chu, *Nanomaterials* **2020**, 12, 2020.
- [69] B. S. NoreMBERG, R. M. Silva, O. G. Paniz, J. H. Alano, J. Dupont, N. L. V. Carreño, *MRS Commun.* **2019**, 9, 726.
- [70] P. Tamailarasan, S. Ramaprabhu, *J. Phys. Chem. C* **2012**, 116, 14179.
- [71] P. Tamilarasan, S. Ramaprabhu, *J. Mater. Chem. A* **2014**, 2, 14054.
- [72] Y. J. Kang, H. Chung, C.-H. Han, W. Kim, *Nanotechnol.* **2012**, 23, 065401.
- [73] C. H. Kim, J.-H. Wee, Y. A. Kim, K. S. Yang, C.-M. Yang, *J. Mater. Chem. A* **2016**, 4, 4763.
- [74] S. K. Simotwo, P. R. Chinnam, S. L. Wunder, V. Kalra, *ACS Appl. Mater. Interfaces* **2017**, 9, 33749.
- [75] Y. Sun, J. Xue, Z. Li, B. Ding, Y. An, S. Zang, H. Dou, J. Jiang, X. Zhang, *J. Electroanal. Chem.* **2021**, 895, 115471.
- [76] A. Eftekhari, *Energy Storage Mater.* **2017**, 9, 47.
- [77] K. O. Oyedotun, T. M. Masikhwa, S. Lindberg, A. Matic, P. Johansson, N. Manyala, *Chem. Eng. J.* **2019**, 375, 121906.
- [78] M.-R. Gao, J. Yuan, M. Antonietti, *Chem. Eur. J.* **2017**, 23, 5391.
- [79] S. Ptak, A. Zarski, J. Kapusniak, *Materials* **2020**, 13, 4479.
- [80] K. R. Seddon, *J. Chem. Technol. Biotechnol.* **1997**, 68, 351.
- [81] L. Sun, H. Zhou, L. Li, Y. Yao, H. Qu, C. Zhang, S. Liu, Y. Zhou, *ACS Appl. Mater. Interfaces* **2017**, 9, 26088.
- [82] J. Cheng, Q. Xu, J. Lu, J. Du, Q. Chen, Y. Zhang, Z. Li, F. He, F. Wu, H. Xie, *Energy Technol.* **2019**, 7, 1800734.
- [83] H. Zhang, Y. Ling, Y. Peng, J. Zhang, S. Guan, *Inorg. Chem. Commun.* **2020**, 115, 107856.
- [84] J. Zhou, L. Bao, S. Wu, W. Yang, H. Wang, *J. Mater. Res.* **2017**, 32, 404.
- [85] S. Cheng, B. Chen, L. Qin, Y. Zhang, G. Gao, M. He, *RSC Adv.* **2019**, 9, 8137.
- [86] Z. Ling, G. Wang, Q. Dong, B. Qian, M. Zhang, C. Li, J. Qiu, *J. Mater. Chem. A* **2014**, 2, 14329.
- [87] A. Chen, Y. Li, L. Liu, Y. Yu, K. Xia, Y. Wang, S. Li, *Appl. Surf. Sci.* **2017**, 393, 151.
- [88] S. Maity, A. A. Vannathan, T. Kella, D. Shee, P. P. Das, S. S. Mal, *Ceram. Int.* **2021**, 47, 27132.
- [89] S. Ma, X. Xu, W. Wu, *ACS Appl. Energy Mater.* **2022**, 5, 3401.
- [90] H. Li, X. Hu, C. Wang, Y. Chen, K. Zhuo, J. Wang, *Int. J. Hydrogen Energy* **2022**, 47, 19195.
- [91] H. Li, X. Hu, Y. Chen, H. Li, G. Bai, K. Zhuo, *J. Phys. Chem. C* **2022**, 126, 9304.
- [92] R. A. Perera Jayawickramage, J. P. Ferraris, *Nanotechnol.* **2019**, 30, 155402.
- [93] X. Lyu, F. Su, M. Miao, *J. Power Sources* **2016**, 307, 489.
- [94] D. W. Lawrence, C. Tran, A. T. Mallajoyula, S. K. Doorn, A. Mohite, G. Gupta, V. Kalra, *J. Mater. Chem. A* **2016**, 4, 160.
- [95] Z. Chen, Z. Li, X. Ma, Y. Wang, Q. Zhou, S. Zhang, *Electrochim. Acta* **2019**, 319, 843.
- [96] H. Pan, Y. Zhang, Y. Pan, W. Lin, W. Tu, H. Zhang, *Chem. Eng. J.* **2020**, 401, 126083.
- [97] B. K. Deka, A. Hazarika, J. Kim, N. Kim, H. E. Jeong, Y.-B. Park, H. W. Park, *Chem. Eng. J.* **2019**, 355, 551.
- [98] J. Liu, L. Ma, Y. Zhao, H. Pan, H. Tang, H. Zhang, *Chem. Eng. J.* **2021**, 411, 128573.
- [99] A. Singh, P. S. Dhapola, S. Singh, P. K. Singh, A. S. Samsudin, N. G. Sahoo, H.-W. Rhee, *High Perform. Polym.* **2020**, 33, 469.
- [100] F. Gao, G. Lewes-Malandrakis, M. T. Wolfer, W. Müller-Sebert, P. Gentile, D. Aradilla, T. Schubert, C. E. Nebel, *Diam. Relat. Mater.* **2015**, 51, 4479.
- [101] J. Liu, X.-W. Mei, F. Peng, *Chin. Chem. Lett.* **2023**, 68, 108187.



**Karamveer Sheoran** is pursuing a doctoral degree (under the supervision of Dr. Samarjeet Singh Siwal and Dr. Vijay Kumar Thakur) at the Department of Chemistry, Maharishi Markandeshwar (deemed to be University) Mullana, Ambala, India. He received his master's degree in chemistry in 2020 from Maharishi Markandeshwar (deemed to be University) Mullana, Ambala, India, and did his bachelor's degree from Kurukshetra University, Kurukshetra, India, in 2018. His current research interest involves material science disciplines, synthesis and applications of sustainable materials and nanocomposites in energy storage and biosensing.



**Harjot Kaur** is pursuing a doctoral degree (under the supervision of Dr. Samarjeet Singh Siwal & Dr. Vijay Kumar Thakur) at the Department of Chemistry, Maharishi Markandeshwar (deemed to be University) Mullana, Ambala, India. She received her bachelor's degree in 2017 from Kurukshetra University, Kurukshetra, India. She did her Master's degree in chemistry from Maharishi Markandeshwar (deemed to be University), Mullana-Ambala, India, in 2020. Her research interests focus on developing nanocomposites and nanotechnologies for enhanced biosensing and renewable energy technologies.



**Samarjeet Singh Siwal** is currently working as an Associate Professor in the Department of Chemistry, MM(DU), Mullana, India. He received his Ph.D. in Chemistry from the University of Johannesburg, South Africa, in 2017. Then, he moved to Kunming University of Science and Technology (KUST), China as a post-doctoral research fellow (in the group of Prof. Qibo Zhang). His research interests include synthesizing and applying 2D materials in different fields, such as overall water splitting, supercapacitors, fuel cells and biosensors. He has published over 70 SCI journal articles, 2 patents, and 5 book chapters.



**Vijay Kumar Thakur** is a Professor and Founding Head of the Biorefining and Advanced Materials Research Centre at SRUC, Edinburgh, UK. Before commencing his tenure at SRUC, he held faculty positions at Cranfield University, Washington State University, USA, and Nanyang Technological University, Singapore. His research activities span the disciplines of Biorefining, Chemistry, Manufacturing, Materials Science, Nanotechnology, and Sustainable and Advanced Materials. He has published over 350 SCI journal articles, 2 patents, 52 books, and 40 book chapters. He sits on the editorial board of several SCI journals as an Editor/Editorial Advisory Board member.